Letters to the Editor

Longitudinal study of a SARS-CoV-2 infection in an immunocompromised patient with X-linked agammaglobulinemia

Dear Editor,

In this journal, Walsh and colleagues[1] recently reviewed the evidence supporting that immunocompromised patients may remain positive for Severe Acute Respiratory Syndrome Coronavirus 2 (SARS-CoV-2) infection for long periods of time, up to 20 days. Here, we report the case of an immunocompromised patient with clinically diagnosed X-linked agammaglobulinemia (XLA) (*Supplementary Material*) who was persistently infected with SARS-CoV-2 for almost five months. He was admitted to the hospital on the 14th April 2020 with left bilobar pneumonia, reporting cough, chronic diarrhoea, and fever over the previous four days, and a nasopharyngeal (NP) sample tested positive for SARS-CoV-2 by RT-qPCR (Fig. 1A). In the hospital, he was treated with hydroxychloroquine, two courses of remdesivir, lopinavir/ritonavir, antibiotics, antifungal treatments, and glucocorticoids. Infectious SARS-CoV-2 was successfully cultured from a bronchoalveolar lavage (BAL) sample on day 50, showing that the virus was actively replicating in the lower respiratory airways (*Supplementary Material*). On day 133, he was treated with hyperimmune serum from a convalescent patient. Despite treatments and two coronavirus disease 2019 test negativizations, the patient stayed in the hospital most of the time and died in the intensive care unit from multiorgan failure and shock on day 149 (10th September 2020) (Fig. 1A). See the *Supplementary Material* for further details.

Throughout the period described, 26 respiratory samples were collected from the patient (22 NP swabs and 4 BAL samples) (Fig. 1A). A urine, faeces, and peripheral blood sample (on day 44), and another peripheral blood sample (on day 87) were collected, but viral genome was not detected in any of their RNA extractions. SARS-CoV-2 viral genomes of a subset of 13 NP and 3 BAL samples were sequenced using alternative methodologies (Supplementary Material). All genomes were assigned to the PANGO lineage A.2 (Clade 19B), which was predominant in Spain during the early months of the pandemic.[2] Assignation of the sequences to the same lineage suggests that the patient had a single viral infection event. Synonymous and non-synonymous mutations accumulated throughout the course of the infection in NP and BAL samples (Spearman correlation, $r = 0.77$, $p = 0.00072$) (Fig. 1B). Different constellations of mutations were observed in the sequences isolated from NP and BAL samples, suggesting compartmentalization of viral subpopulations evolving independently. The median mutation rate -accumulated mutations per day since diagnosis- was 0.09 mutations/day, higher than the originally estimated for SARS-CoV-2 (0.06 mutations/day[3]) (One-sample Wilcoxon test, $p = 0.005$), indicating accelerated mutation rate

during infection. There was no significant difference in the mutation rate calculated for NP and BAL samples (Mann-Whitney U test, $p = 0.18$).

On day 0, viral genome sequences harboured the characteristic mutational pattern of lineage A.2 (ORF1a:F3701Y, ORF3a:G196V, ORF8:L84S, N:S197L) in addition to two other substitutions and four synonymous mutations (Fig. 1B). In particular, the spike (S) gene sequence was characterized by the I197V substitution and one synonymous mutation. These were the only two mutations observed in the S gene throughout the course of this five-month infection period in NP samples. However, we observed a different evolutionary pattern in BALs. On day 50, the A653V substitution was observed. This was found as part of the mutational pattern of two variants spreading in France[4] and Germany[5] at the beginning of 2021. On day 87, the P384L in the receptor-binding domain emerged but disappeared together with the A653V at day 136, five days after treatment with hyperimmune serum, when R158S and N501T emerged. Strikingly, the N501T is associated with an increased binding affinity of the S protein to the human angiotensin-converting enzyme 2 (ACE2) receptor and has been identified as an escape mutation against anti-SARS-CoV-2 neutralizing antibodies (NAbs).[6] Interestingly, the position R158 of the S protein is part of the N-terminal domain (NTD) antigenic supersite, a region being recognized by all known NAbs directed to the NTD,[7] and the R158S has been included among the escape mutations of anti-SARS-CoV-2 monoclonal NAbs targeting the NTD of the S protein.[8] Besides, we highlight the emergence, on day 50, of the G204R in the nucleocapsid (N) gene, a mutation characteristic of the P.2 lineage, and, on day 136, of the K1795Q in the ORF1a and the P67S in the N gene, which are distinctive signatures of P.1 and B.1.617.3 lineages, respectively.

This study describes an XLA-immunocompromised patient with prolonged SARS-CoV-2 infection, supporting evidence that these patients undergo viral shedding for long periods of time.[9,10] The patient presented RT-qPCR negative NP samples in different time intervals throughout the course of infection that either matched to a positive BAL sample or were followed by a positive RT-qPCR sample. This indicates that a negative RT-qPCR result in NP samples may not imply remission from infection.[9] Viral genome sequencing revealed an accelerated intra-host viral evolution. Different mutations were accumulated in samples collected from NPs and BALs throughout the course of infection, which may point to viral adaptation to the upper and lower respiratory airways. Several host factors may account for this phenomenon, such as temperature and immune response disparities and/or differences in the ACE2 expression. Furthermore, it is worth noting that the mutations emerging in the lower respiratory tract were not detected by sequencing NP samples. Thus, the emergence of potentially worrying viral variants may be underestimated by sequencing standards focusing on NP samples. The emergence of substitutions linked to
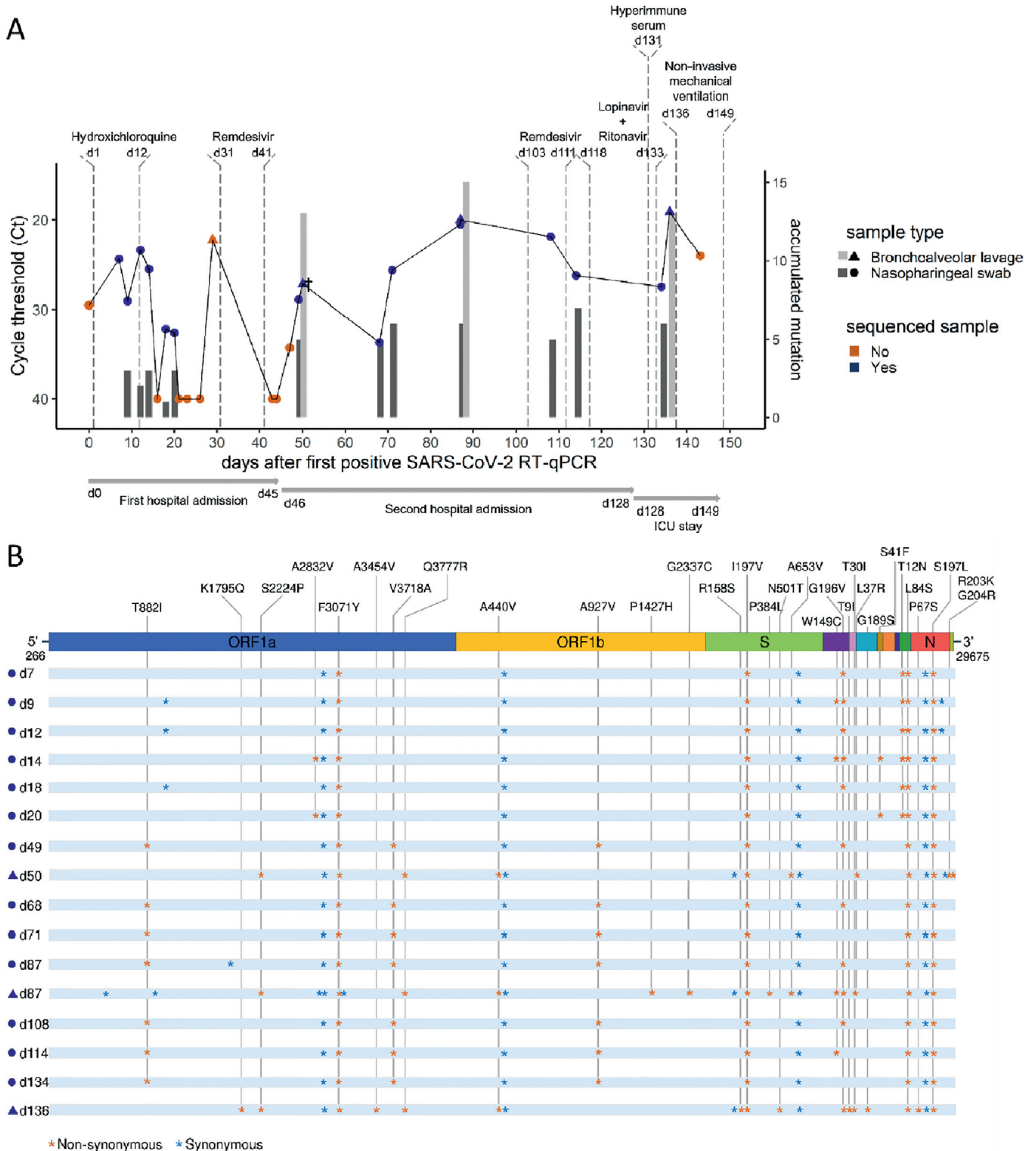
Fig. 1. *Five-month longitudinal study of SARS-CoV-2 positive samples collected from a XLA-immunocompromised patient.* **(A)** Chronological visualization of samples collected throughout the course of infection until patient death (day 149). RT-qPCR cycle threshold (Ct) are shown for collected nasopharyngeal swab (NP, circle) and bronchoalveolar (BAL, triangle) samples, with sequenced samples highlighted in blue. Vertical bars represent the accumulated number of mutations in the sequenced genome compared to the consensus viral sequence obtained from the first NP sample (day 9). † At day 50, a BAL sample was shown to have actively replicating SARS-CoV-2 viruses. **(B)** Graphical representation of SARS-CoV-2 whole-genome consensus sequences with synonymous (blue asterisks) and nonsynonymous mutations (orange asterisks) identified as compared to the Wuhan-Hu-1 reference sequence (NC_045512.2). Only non-synonymous mutations are identified with the amino acid changes in the figure. On day 50, in the N gene, the amino acid substitution S197L is replaced by S197T. (For interpretation of the references to colour in this figure legend, the reader is referred to the web version of this article)

immune evasion in the BAL sample collected three days after treatment with hyperimmune serum is remarkable. Of note, the presence of the same or other mutations of interest in the NP samples days after hyperimmune serum treatment could not be ruled out. In fact, we were able to sequence only one NP sample 24 h after treatment, which may not be enough time to observe a possible viral population shifting in these samples. One limitation is that we have no data on the Abs composition and SARS-CoV-2 neutralizing activity of the hyperimmune serum used. Lastly, the emergence of mutations distinctive of currently circulating SARS-CoV-2 variants of concern (VOCs) support the hypothesis for long-term viral shedding in immunocompromised patients as one possible mechanism for the emergence of VOCs.

Declaration of Competing Interest

The authors declare that they have no known competing financial interests or personal relationships that could have appeared to influence the work reported in this paper.

Ethical approval

The University Hospital Nuestra Señora de Candelaria (Santa Cruz de Tenerife, Spain) review board approved the study (ethics approval number: CHUNSC_2020_24).

Authors Contribution

JAF and CF conceived the idea, the experimental design and supervised the project. LC, JMLS, HRP, HGC, AIC, RGM, and DGMA conducted the sequencing experiments. SRA and MEAA conducted the viral culture experiments. MHP, JAF, HGC, ODG, and DGMA collected patient data. LC, JMLS, AVF, and CF performed the analysis and interpreted the results. AVF and CFA obtained the funding. LC

drafted the first version of the manuscript and prepared the figures. All authors contributed to manuscript revision and read and approved the submitted version.

Supplementary materials

Supplementary material associated with this article can be found, in the online version, at doi:10.1016/j.jinf.2021.07.028.

References

1. Walsh K.A., Spillane S., Comber L., Cardwell K., Harrington P., Connell J., et al. The duration of infectiousness of individuals infected with SARS-CoV-2. *J Infect [Internet]*. 2020 Dec 1;**81**(6):847–56. Available from https://doi.org/10.1016/j.jinf.2020.10.009.
2. Latif A.A, Mullen J.L, Alkuzweny M, Tsueng G, Cano M, Haag E, et al. A.2 Lineage report [Internet]. outbreak.info. 2021 [cited 2021 Jun 21]. Available from: https://outbreak.info/situation-reports?pango=A.2.
3. Harvey W.T. Carabelli A.M., Jackson B., Gupta R.K., Thomson E.C., Harrison E.M., et al. SARS-CoV-2 variants, spike mutations and immune escape. *Nat Rev Microbiol [Internet]*. 2021;**19**(7):409–24. Available from https://doi.org/10.1038/s41579-021-00573-0.
4. Colson P., Levasseur A., Delerce J., Pinault L., Dudouet P., Devaux C., et al. Spreading of a new SARS-CoV-2 N501Y spike variant in a new lineage. *Clin Microbiol Infect [Internet]*. 2021 Jun 9. Available from https://doi.org/10.1016/j.cmi.2021.05.006.
5. Mallm J.P., Bundschuh C., Kim H., Weidner N., Steiger S., Lander I., et al. Local emergence and decline of a SARS-CoV-2 variant with mutations L452R and N501Y in the spike protein. *medRxiv [Internet]*. 2021. Available from: https://www.medrxiv.org/content/early/2021/04/29/2021.04.27.21254849.
6. Wang R., Chen J., Gao K., Wei G.W.. Vaccine-escape and fast-growing mutations in the United Kingdom, the United States, Singapore, Spain, India, and other COVID-19-devastated countries. *Genomics [Internet]*. 2021;**113**(4):2158–70. Available from https://www.sciencedirect.com/science/article/pii/S0888754321001798.
7. McCallum M., De Marco A., Lempp F.A., Tortorici M.A., Pinto D., Walls A.C., et al. N-terminal domain antigenic mapping reveals a site of vulnerability for SARS-CoV-2. *Cell [Internet]*. 2021 Apr 29;184(9):2332–2347.e16. Available from: https://doi.org/10.1016/j.cell.2021.03.028
8. Suryadevara N., Shrihari S., Gilchuk P., VanBlargan L.A., Binshtein E., Zost S.J., et al. Neutralizing and protective human monoclonal antibodies recognizing the N-terminal domain of the SARS-CoV-2 spike protein. *Cell [Internet]*. 2021 Apr 29;**184**(9). 2316–2331.e15. Available from https://doi.org/10.1016/j.cell.2021.03.029.
9. Choi B., Choudhary M.C., Regan J., Sparks J.A., Padera R.F., Qiu X., et al. Persistence and evolution of SARS-CoV-2 in an immunocompromised host. *N Engl J Med [Internet]*. 2020 Dec 3 [cited 2021 Feb 17];**383**(23):2291–3. Available from: http://www.nejm.org/doi/10.1056/NEJMc2031364.
10. Baang J.H., Smith C., Mirabelli C., Valesano A.L., Manthei D.M., Bachman M.A., et al. Prolonged severe acute respiratory syndrome coronavirus 2 replication in an immunocompromised patient. *J Infect Dis [Internet]*. 2021 Jan 1;**223**(1):23–7. Available from https://doi.org/10.1093/infdis/jiaa666.

Laura Ciuffreda[1]
Research Unit, Hospital Universitario Nuestra Señora de Candelaria, Spain

José M. Lorenzo-Salazar[1]
Genomics Division, Instituto Tecnológico y de Energías Renovables, Spain

Julia Alcoba-Florez[1]
Servicio de Microbiología, Hospital Universitario Nuestra Señora de Candelaria, Spain

Héctor Rodriguez-Pérez
Research Unit, Hospital Universitario Nuestra Señora de Candelaria, Spain

Helena Gil-Campesino
Servicio de Microbiología, Hospital Universitario Nuestra Señora de Candelaria, Spain

Antonio Íñigo-Campos
Genomics Division, Instituto Tecnológico y de Energías Renovables, Spain

Diego García-Martínez de Artola

Servicio de Microbiología, Hospital Universitario Nuestra Señora de Candelaria, Spain

Agustín Valenzuela-Fernández
Laboratorio de Inmunología Celular y Viral, Unidad de Farmacología, Facultad de Medicina, Universidad de La Laguna, Spain; Red española de Investigación en VIH/SIDA (RIS)-RETIC, Instituto de Salud Carlos III, Spain

Marcelino Hayek-Peraza
Servicio de Medicina Interna, Hospital Universitario Nuestra Señora de Candelaria, Spain

Susana Rojo-Alba, Marta Elena Alvarez-Argüelles
Servicio de Microbiología, Hospital Universitario Central de Asturias, Spain

Oscar Díez-Gil
Servicio de Microbiología, Hospital Universitario Nuestra Señora de Candelaria, Spain

Rafaela González-Montelongo
Genomics Division, Instituto Tecnológico y de Energías Renovables, Spain

Carlos Flores*
Research Unit, Hospital Universitario Nuestra Señora de Candelaria, Spain
Genomics Division, Instituto Tecnológico y de Energías Renovables, Spain
CIBER de Enfermedades Respiratorias, Instituto de Salud Carlos III, Spain

*Corresponding author.
E-mail address: cflores@ull.edu.es (C. Flores)

[1] Should be considered co-first authors.

Avian influenza H10 subtype viruses continuously pose threat to public health in China

Dear editor,

Wang and colleges recently reported in this journal the first case of human infection with H10N3 virus in China.[1] In China, H10 subtype (H10N2, H10N3, H10N6, H10N7, H10N8, and et. al.) avian influenza virus (AIV) had distributed in poultry and wild bird populations in China.[2] Because poultry showed no clinical symptoms when infected with H10 subtype viruses, their eradication had not been a priority for the control of zoonosis diseases in China. However, H10 subtype viruses had continuously contributed to some zoonotic spillover events. In 2010, a number of cases of human infected with H10N7 were reported in Australia[2], and subsequently, China reported that the first human case of H10N8 infection that resulted in a human death in 2013 and the recently emerged human-infecting H10N3 virus in 2021.[1,3] Therefore, the H10 subtype AIV poses continuous public health concerns. To that purpose, we systematically analyzes the evolutionary dynamics and dissemination pathways of H10 subtype AIV in China.

In the present study, to elucidate the evolutionary process of H10 subtype influenza viruses, we firstly examined HA genes of global H10 subtype virus by performing multiple sequence alignment and phylogenetic analysis.[3,4] H10 subtype viruses had divided into two lineages—North American-lineage and Eurasian-lineage (Fig. 1A). We observed that the H10 subtype viruses in Eurasian-lineage were more complex embodying different neuraminidases, while the H10N7 virus was concentrated on North American-lineage (Fig. 1A). All of the H10 subtype viruses isolated from China were derived from Eurasian-lineage. It is interesting to note that 78.5% of the H10 subtype viruses (N2-N9) were isolated from Jiangxi province (Fig. 1B–D), indicating that Jiangxi province of China is the epicenter of the H10 subtype viruses. In addition, we also found that the number of H10 subtype viruses increased during 2000–2015, and subsequently decreased after 2016 (Fig. 1B). The H10N3 and H10N8 influenza viruses exhibited the highest number of H10 subtype virus in China. H10N8 virus had become the dominant subtype in poultry during 2011–2015; however, the number of H10N3 virus had increased during 2016–2021 (Fig. 1B), indicative of dominant H10 subtype switch in China. Previous study showed that genetic diversity of H10N8 viruses were much higher prior to human spillover event.[2] In this study, we found that the genetic diversity of human-origin H10N3 viruses were lower than that of H10N8 viruses (Supplementary Fig. 1), and we also found that the genotype of human-infecting H10N3 virus was same as the A/chicken/Jiangsu/0110/2019(H10N3) and A/chicken/Jiangsu/0104/2019(H10N3). These findings supported the finding that the avian-to-human transmission of H10N3 virus might have occurred recently without further reassortment.

To estimate the population dynamics of H10 subtype influenza virus in China, we inferred the HA genes of H10 subtype virus demographic history using Bayesian Skyride plots (Supplementary Fig. 2). Our finding suggested that from 2012 to 2014, the decreasing effective population size indicated that the diversity of H10 subtype viruses declined, while genetic diversity increased dramatically during 2014 to 2015 and then stably maintained (Fig. 2A and B). Subsequently, we analyzed the dissemination pathways of H10 subtype viruses in China in different sampling locations based on the HA phylogenetic tree. Among the result, we found that Jiangxi province was regarded as epicenter for the viral spread (Fig. 2C). Specifically, Jiangxi was linked with three locations—Hunan, Hubei, and Hebei. In addition, we found that Zhejiang was linked with closer province including Jiangsu(Fig. 2C). However, there are some limitations that sampling bias might have affected the results. Among our findings, the transmission routes of H10 subtype viruses were primarily concentrated in Jiangxi province of China. Previous study showed that the role of wild birds in the dispersal of AIVs during the seasonal migration.[5,6,7] In the case of Jiangxi province, the Poyang Lake, with its excellent ecology and vast wetlands, has become a world-famous migratory bird wintering hub, which increase the close contact between wild birds carrying H10 subtype viruses and poultry, accelerating the reassortment and mammalian adaptive mutations.

The emerged H10N3 and H10N8 influenza viruses had caused human infection in China, posing public health threat. In previous study, we found that the key substitutions in PB2 protein of H10N8 viruses including I292V, A588V, and T598M were associated with mammalian adaption.[8,9] Thus, a key concern is whether the H10 subtype viruses in poultry had acquired the mammalian adaption in recent years. In the present study, we found that the proportion of I292V, A588V, and T598M substitutions in the PB2 protein of H10 subtype viruses in poultry increased sharply during 2013 to 2021 (Fig. 2D), and the human-infecting H10N3 and H10N8 viruses all harbored these amino acids substitutions, indicating that H10 subtype viruses in China pose an increasing threat to hu-
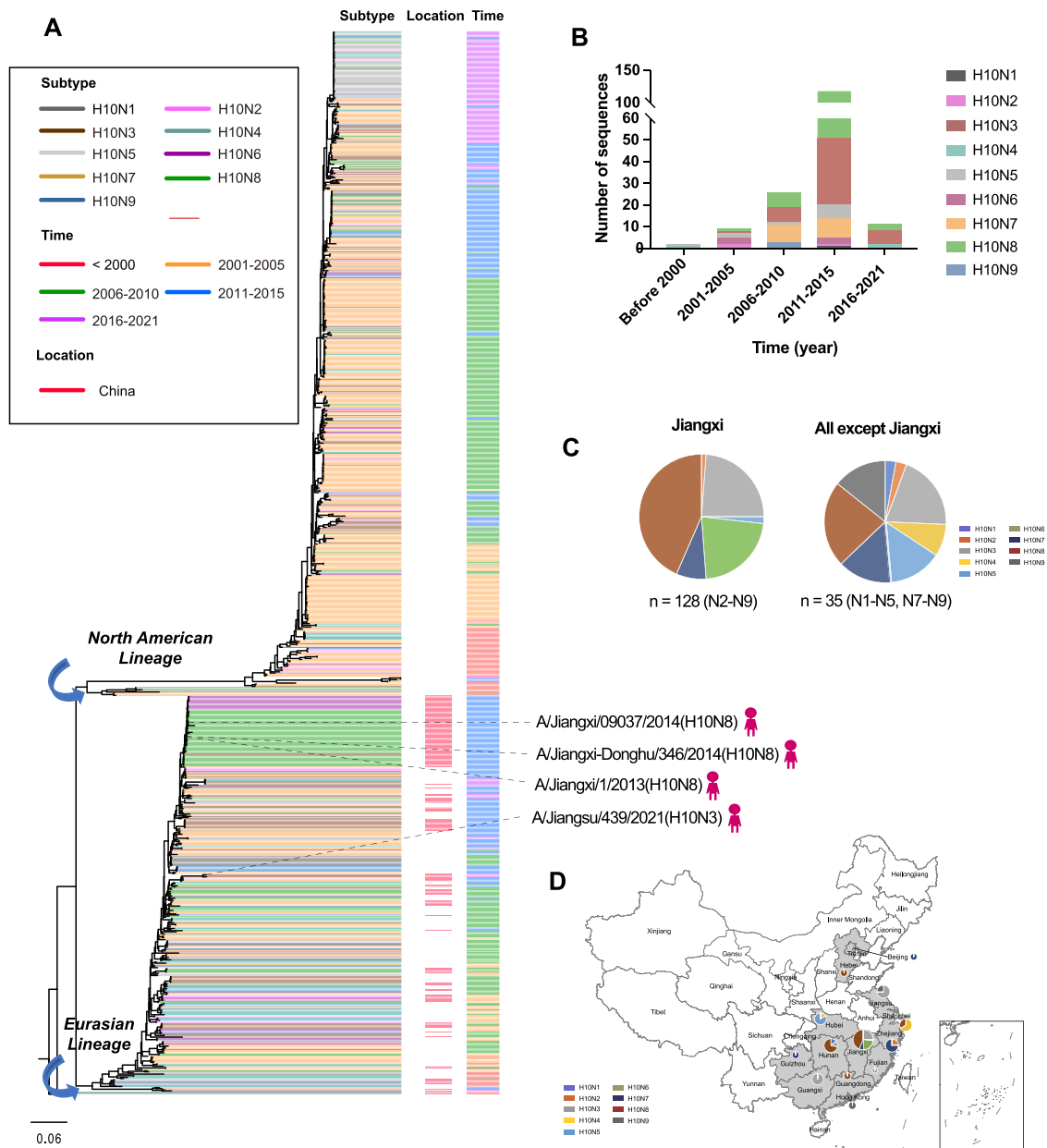
Fig. 1. Geographic distribution and evolutionary history of H10 subtype influenza viruses. **(A)** Maximum likelihood tree of HA gene sequences of H10Nx viruses. All branch lengths are scaled according to the numbers of substitutions per site (subs/site). Maximum likelihood (ML) phylogenies for the codon alignment of the full gene segments were estimated using the GTRGAMMA nucleotide substitution model in the IQ-tree. Node support was determined by nonparametric bootstrapping with 1000 replicates. The phylogenetic tree was visualized in the FigTree (version 1.4.3) program. **(B)** The number of sequences of different H10Nx viruses in China. **(C)** The distribution of H10Nx influenza viruses in China embodying different NA genes in Jiangxi and all except Jiangxi. **(D)** The geographic distribution of H10 subtype viruses in China. The size of the pie chart represents the number of H10 subtype viruses in China, and the different color represents the H10 subtype embodying different NA genes. Data are available from GISAID's Epiflu Database.

man health. H10 subtype viruses had been detected in migratory birds in China with increasing trend and H10 subtype viruses were more adapted to mice and chickens[2,8], which signal a very real risk that wild bird migration might probable introduce H10 subtype viruses associated with mammalian adaption to other countries, posing global public health concerns.

In conclusion, our findings suggested that H10N3 and H10N8 AIVs had been co-circulating in poultry population in China, and many molecular markers in PB2 protein associated to mammalian adaption had been detected in bird- and human-origin H10 subtype AIV. Notably, we also found that Jiangxi province of China is

the main output region in the dissemination of H10 viruses, indicating that eastern China is the potential epicenter of the H10 influenza viruses. Whether H10 subtype AIV could be spread in other countries and circulated via wild bird migration, comprehensive surveillance is warranted to prevent the potential for the future influenza pandemics.

Declaration of Competing Interest

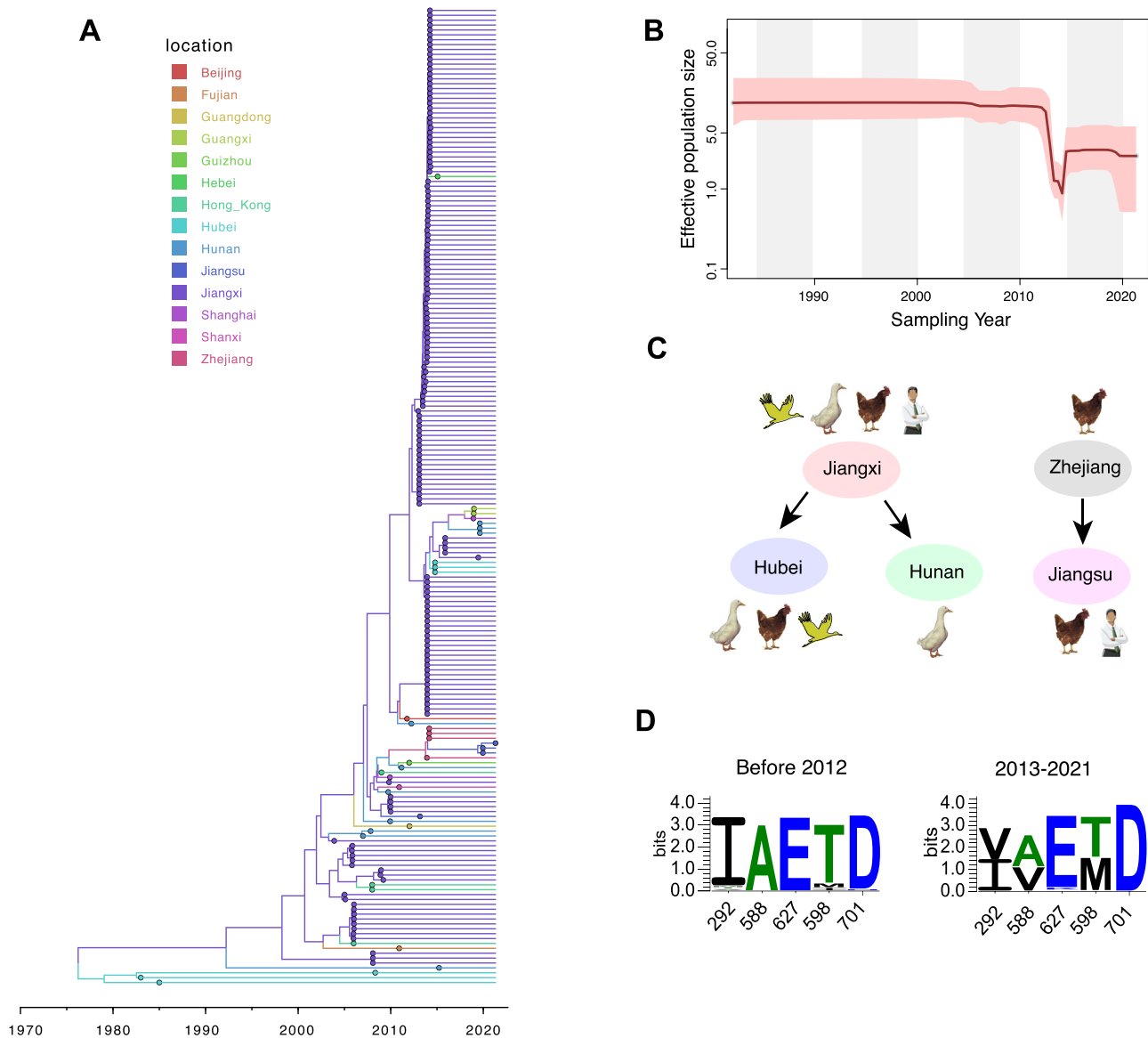All authors have no potential conflicts of interest to disclose.

Fig. 2. Evolutionary and transmission dynamics of H10Nx influenza viruses. **(A)** MCC tree of H10 subtype viruses in China. **(B)** Bayesian Skyride plot of HA genes of H10 subtype viruses in China. A Bayesian Skyride analysis of HA gene of H10 subtype viruses to display changes in the effective population size over time. The solid red line indicates the median value, and the shaded red area represents the 95% highest posterior density of genetic diversity estimates. **(C)** The transmission routes of H10 subtype viruses in Jiangxi, Hunan, Hubei, Jiangsu, and Zhejiang provinces of China. **(D)** Amino acids frequency of H10 subtype influenza viruses in China. Frequencies of each position, including 292, 588, 598, 627, and 701 in PB2 protein, are illustrated using Weblogo 3.4 (http://weblogo.threeplusone.com/).

Acknowledgments

Supplementary materials

Supplementary material associated with this article can be found, in the online version, at doi:10.1016/j.jinf.2021.07.039.

References

1. Wang Y., Niu S., Zhang B., Yang C., Zhou Z. The whole genome analysis for the first human infection with H10N3 influenza virus in China. *J Infect*; 2021. doi:10.1016/j.jinf.2021.06.021.
2. Wu H., Yang F., Liu F., Peng X., Chen B., Cheng L., et al. Molecular characterization of H10 subtype avian influenza viruses isolated from poultry in Eastern China. *Arch Virol* 2019;**164**:159–79.
3. Qi W., Zhou X., Shi W., Huang L., Xia W., Liu D., et al. Genesis of the novel human-infecting influenza A(H10N8) virus and potential genetic diversity of the virus in poultry, China. *Euro Surveill* 2014;**19**:20841. doi:10.2807/1560-7917.
4. Katoh K., Misawa K., Kuma K., Miyata T.. MAFFT: a novel method for rapid multiple sequence alignment based on fast Fourier transform. *Nucleic Acids Res* 2002;**30**:3059–66.
5. Nguyen L.T., Schmidt H.A., von Haeseler A., Minh B.Q. IQ-TREE: a fast and effective stochastic algorithm for estimating maximum-likelihood phylogenies. *Mol Biol Evol* 2015;**32**:268–74.
6. Hill S.C., Lee Y.J., Song B.M., Kang H.M., Lee E.K., Hanna A., et al. Wild waterfowl migration and domestic duck density shape the epidemiology of

highly pathogenic H5N8 influenza in the Republic of Korea. *Infect Genet Evol* 2015;**34**:267–77.

7. Fusaro A., Zecchin B., Vrancken B., Abolnik C., Ademun R., Alassane A., et al. Disentangling the role of Africa in the global spread of H5 highly pathogenic avian influenza. *Nat Commun* 2019;**10**:5310.

8. Xiao C., Ma W., Sun N., Huang L., Li Y., Zeng Z., et al. PB2-588V promotes the mammalian adaptation of H10N8, H7N9 and H9N2 avian influenza viruses. *Sci Rep* 2016;**6**:19474.

9. Li B., Su G., Xiao C., Zhang J., Li H., Sun N., et al. The PB$_2$ co-adaptation of H10N8 avian influenza virus increases the pathogenicity to chickens and mice. *Transbound Emerg Dis* 2021. doi:10.1111/tbed.14157.

Jiahao Zhang[1]

College of Veterinary Medicine, South China Agricultural University, Guangzhou 510642, PR China

National Avian Influenza Para-reference Laboratory, Guangzhou 510642, PR China

National and Regional Joint Engineering Laboratory for Medicament of Zoonoses Prevention and Control, National Development and Reform Commission of the People's Republic of China, Guangzhou 510642, PR China

Key Laboratory of Zoonoses, Ministry of Agricultural and Rural Affairs of the People's Republic of China, Guangzhou 510642, PR China

Lihong Huang[1]

Department of Biomedical Sciences, City University of Hong Kong, Hong Kong 999077, PR China

Yiqun Chen, Xiaomin Wang

College of Veterinary Medicine, South China Agricultural University, Guangzhou 510642, PR China

National Avian Influenza Para-reference Laboratory, Guangzhou 510642, PR China

National and Regional Joint Engineering Laboratory for Medicament of Zoonoses Prevention and Control, National Development and Reform Commission of the People's Republic of China, Guangzhou 510642, PR China

Key Laboratory of Zoonoses, Ministry of Agricultural and Rural Affairs of the People's Republic of China, Guangzhou 510642, PR China

Ming Liao*, Wenbao Qi*

College of Veterinary Medicine, South China Agricultural University, Guangzhou 510642, PR China

National Avian Influenza Para-reference Laboratory, Guangzhou 510642, PR China

Guangdong Laboratory for Lingnan Modern Agriculture, Guangzhou 510642, PR China

National and Regional Joint Engineering Laboratory for Medicament of Zoonoses Prevention and Control, National Development and Reform Commission of the People's Republic of China, Guangzhou 510642, PR China

Key Laboratory of Zoonoses, Ministry of Agricultural and Rural Affairs of the People's Republic of China, Guangzhou 510642, PR China

Key Laboratory of Animal Vaccine Development, Ministry of Agricultural and Rural Affairs of the People's Republic of China, Guangzhou 510642, PR China

Key Laboratory of Zoonoses Prevention and Control of Guangdong Province, Guangzhou 510642, PR China

*Corresponding authors at: College of Veterinary Medicine, South China Agricultural University, Guangzhou 510642, PR China.
E-mail addresses: mliao@scau.edu.cn (M. Liao), qiwenbao@scau.edu.cn (W. Qi)

[1] These authors contributed equally to this work.
Accepted 31 July 2021

Stool culture for diagnosis of nontuberculous mycobacteria pulmonary disease: An indirect evidence

Dear editor,

We agree with Tan and colleagues, who described the situation of Nontuberculous mycobacteria (NTM) pulmonary diseases (NTM-PDs) in China [1]. NTM-PD remain difficult to be managed even with several guidelines [2]. This is because that NTM-PD infections usually share some symptoms with pulmonary tuberculosis (TB), and most of NTM species are resistant to first-line anti-TB agents. In addition, mycobacterial culture and identification of NTM are not routinely performed in most areas, such as China. These make the diagnosis and treatment of NTM disease more complicated and may contribute to a poor outcome.

Certainly, the rapid identification would aid to improve the management of NTM-PD patients. According to a guideline issued recently, positive culture results from at least two separate expectorated sputum samples is known as one of the microbiologic criteria for the NTM-PD diagnosis [3]. Stools, as an alternative to sputum, have been well characterized in the diagnosis of pulmonary TB, especially in children [4-6]. However, the role of stool samples for the diagnosis of NTM-PD remains unclear.

In this retrospective study, we hypothesized that stool samples may be useful for NTM-PD diagnosis. To test this hypothesis, we reviewed our experience of stool cultures for NTM species over the last decades. Fortunately, some interesting findings were found, which could be taken as an indirect evidence for NTM-PD diagnosis using stool samples.

This study was conducted at the Shandong Public Health Clinical Center and confronted with the Helsinki Declaration. The study protocol was approved by the Ethical Committee of Shandong Public Health Clinical Center. Due to the retrospective nature of the study and the anonymous data analyzed, our study was waived for written informed consent by the Ethical Committee of Shandong Public Health Clinical Center. Shandong Public Health Clinical Center is a provincial referral hospital of infectious diseases (including TB), with approximately 2000 beds.

Between January 2012 and August 2020, consecutive patients with positive mycobacterial cultures were included for analysis. Mycobacterial culture was performed using Löwenstein-Jensen medium method, when NTM disease was suspected, further identification was performed using the Mycobacteria Identification Array Kit (CapitalBio, Beijing, China), or sequencing of 16S rDNA. NTM disease was diagnosed according to ATS/IDSA criteria [7]. Continuous data were presented as mean ± standard deviation (SD) and categorical data were presented as count (percentages).

Between May 2012 and June 2021, mycobaterial strains were isolated from 25,617 samples. Of them, 1107 (4.3%) strains were identified as NTM species, including 110 strains isolated from outpatients. Therefore, a total of 997 strains isolated from inpatients were included for the final analysis.

The samples employed for NTM cultures included: sputum ($n = 925, 92.8\%$), bronchial brushing ($n = 31$, 3.1%), tissues ($n = 12$, 1.2%), stool ($n = 11$, 1.1%), pleural effusion ($n = 9$, 0.9%), urine ($n = 5$, 0.5%), and bronchial alveolar lavage fluid (BALF, $n = 4$,

0.4%). Of the 997 strains, 662 (66.4%) strains were confirmed as *M. intracellulare*, followed by *M. kansasii* ($n = 111$, 11.1%), *M. chelonei* ($n = 103$, 10.3%), *M. fortuitum* ($n = 39$, 3.9%), *M. gordonae* ($n = 20$, 2.0%), *M. avium* ($n = 20$, 2.0%), and others ($n = 42$, 4.2%).

The 11 stool samples were collected from 10 patients. The mean age of them was 42.8 ± 18.2 years old and 60% of them were male. The 11 strains included *M. intracellulare* ($n = 6$), *M. kansasii* ($n = 4$), and *M. avium* ($n = 1$). Of the ten patients, eight have met ATS/IDSA criteria for NTM-PD, including clinical symptoms, radiologic features, and microbiologic evidence obtained from at least two separate sputum samples ($n = 9$), one have intestinal infection confirmed with tissue culture, and the remaining one have confirmed NTM-PD and possible intestinal infection. Therefore, an indirect evidence for NTM-PD diagnosis using stool samples was found in this study, and NTM strains isolated from stool samples support the diagnosis of NTM-PD. In addition, the initial symptoms at admission included cough ($n = 5$), fever ($n = 4$), hemoptysis ($n = 3$), chest pain ($n = 3$), diarrhea ($n = 2$), and dyspnea ($n = 1$).

In the current study, the results of the stool culture method reflect a high level of agreement similar to that of the sputum culture-based determination of NTM-PD, indicating that the stool culture assay reliably identified strains of NTM species. This interesting finding implied that stool is an alternative to sputum for NTM-PD diagnosis. It was demonstrated that stool culture is a useful method for the detection of swallowed NTM species for the diagnosis of patients with NTM-PD.

Diagnosis of NTM-PD usually requires the isolation of NTM species in respiratory samples (such as sputum) [2]. However, the diagnosis may turn to be difficult when patients cannot produce sputum, particularly in younger children or HIV-positive patients [8,9]. Due to a relative immunodeficiency, sputum production may therefore be reduced by a diminished inflammatory response in these subjects [10]. Other specimens collected by invasive procedures, such as bronchial brushing and BALF, may be then employed. When collected, these specimens typically have a low bacterial burden, resulting in modest detection by current available assays. Although multiple specimens improves the detection yield, it is costly and requires consecutive days [11,12].

Most sputum is swallowed, and NTM strains can survive within the intestinal tract [13]. Therefore, stool samples can be used for detecting NTM species originating from the lungs. Besides, stool culture testing may be taken as a tool for the evaluation of responses to empirical treatment for TB diseases [5], this is because the test results for follow-up samples have considerable clinical relevance.

All patients in this study had proven NTM-PD, and only two of them had gastrointestinal symptoms that suggested a coexistent diagnosis of NTM intestinal infections. As known, stool culture can support the diagnosis of NTM intestinal infections. It is possible that in such cases in the present study, this may contribute to the presence of NTM species in the stool [14,15]. However, one of the two patients also had pulmonary symptoms (such as cough and sputum), and another one was confirmed with tissue culture and only had gastrointestinal symptoms. In general, the strong association that we identified between sputum and stool findings among patients with pulmonary symptoms strongly suggests that strains detected in the stool culture could originate from swallowed sputum, and intestinal disease is not the only source.

Our study has several limitations. First, due to the retrospective nature, sample selection bias may arise and affect the final estimates. Second, the cause of the false-negative stool culture results was not investigated. Third, in the study, a single stool sample was collected for mycobacterial culture. If successive daily samples were used, it may be helpful to improve the diagnosis of NTM-PD directly. In addition, we need to determine whether stool culture would provide additional diagnostic value in patients who are unable to expectorate, especially in children and HIV-positive patients.

The data presented herein indicate that stool culture is favourable for the diagnosis of NTM-PD, and patients who are unable to expectorate sputum, such as patients with younger age, impaired mental, and immunocompromised status, could benefit from this alternative method for the NTM-PD diagnosis. However, currently, stool culture for NTM-PD diagnosis cannot be recommended to replace sputum culture. Further studies are required to investigate its role in a prospective way.

Funding

Declaration of Competing Interest

The authors declare no conflict of interest.

Acknowledgements

References

1. Tan Y., Deng Y., Yan X., Liu F., Tan Y., Wang Q., et al. Nontuberculous mycobacterial pulmonary disease and associated risk factors in China: a prospective surveillance study. *J Infect* 2021;**83**:46–53.
2. Daley C.L., Iaccarino J.M., Lange C., Cambau E., Wallace R.J., Andrejak C., et al. Treatment of nontuberculous mycobacterial pulmonary disease: an official ATS/ERS/ESCMID/IDSA clinical practice guideline. *Eur Respir J* 2020;**56**.
3. Daley C.L., Iaccarino J.M., Lange C., Cambau E., Wallace R.J., Andrejak C., et al. Treatment of nontuberculous mycobacterial pulmonary disease: an official ATS/ERS/ESCMID/IDSA clinical practice guideline. *Clin Infect Dis* 2020;**71**:905–13.
4. Nicol M.P., Spiers K., Workman L., Isaacs W., Munro J., Black F., et al. Xpert MTB/RIF testing of stool samples for the diagnosis of pulmonary tuberculosis in children. *Clin Infect Dis* 2013;**57**:e18–21.
5. DiNardo A.R., Kay A.W., Maphalala G., Harris N.M., Fung C., Mtetwa G., et al. Diagnostic and treatment monitoring potential of a stool-based quantitative polymerase chain reaction assay for pulmonary tuberculosis. *Am J Trop Med Hyg* 2018;**99**:310–16.
6. Kokuto H., Sasaki Y., Yoshimatsu S., Mizuno K., Yi L., Mitarai S.. Detection of mycobacterium tuberculosis (MTB) in fecal specimens from adults diagnosed with pulmonary tuberculosis using the Xpert MTB/rifampicin test. *Open Forum Infect Dis* 2015;**2** ofv074.
7. Griffith D.E., Aksamit T., Brown-Elliott B.A., Catanzaro A., Daley C., Gordin F., et al. An official ATS/IDSA statement: diagnosis, treatment, and prevention of nontuberculous mycobacterial diseases. *Am J Respir Crit Care Med* 2007;**175**:367–416.
8. Sabur N.F., Esmail A., Brar M.S., Dheda K.. Diagnosing tuberculosis in hospitalized HIV-infected individuals who cannot produce sputum: is urine lipoarabinomannan testing the answer? *BMC Infect Dis* 2017;**17**:803.
9. Berti E., Galli L., Venturini E., de Martini M., Chiappini E.. Tuberculosis in childhood: a systematic review of national and international guidelines. *BMC Infect Dis* 2014;**14**(1):S3 Suppl.
10. Tarzi M.D., Grigoriadou S., Carr S.B., Kuitert L.M., Longhurst H.J.. Clinical immunology review series: an approach to the management of pulmonary disease in primary antibody deficiency. *Clin Exp Immunol* 2009;**155**:147–55.
11. Sun D-F, Zheng L-L, Jin F., Wang M.-.S. Evaluation of the double sputum Xpert tests for the diagnosis of pulmonary tuberculosis. *Infect Dis* 2019:1–2.
12. Wang Y.N., Han C., Wang J.L., Wang M.S.. Diagnostic accuracy of three morning sputum versus standard sputum smears for pulmonary tuberculosis. *J Investig Med* 2018;**66**:e5.
13. Kobayashi Y., Takano T., Hirayama N., Sato N., Shimoide H.. Isolation of nontuberculous mycobacteria during colonoscopy. *Kekkaku* 1995;**70**:629–34.
14. Tortoli E., Rindi L., Goh K.S., Katila M.L., Mariottini A., Mattei R., et al. Mycobacterium florentinum sp. nov., isolated from humans. *Int J Syst Evol Microbiol* 2005;**55**:1101–6.
15. Colebunders R., Nembunzu M., Portaels F., Lusakumunu K., Kapita B., Piot P.. Isolation of mycobacteria from stools and intestinal biopsies from HIV seropositive and HIV seronegative patients with and without diarrhea in Kinshasa, Zaire. Preliminary results. *Ann Soc Belg Med Trop* 1990;**70**:303–9.

Yu He

Department of Clinical Laboratory, First Affiliated Hospital of Guangxi Medical University, Nanning 530012, China

Yan-An Zhang*

Department of Cardiovascular Surgery, Shandong Public Health Clinical Center, Cheeloo College of Medicine, Shandong University, 46# Lishan Road, Jinan 250013, China
Shandong Key Laboratory of Infectious Respiratory Disease, Jinan, Shandong, China

Mao-Shui Wang*

Shandong Key Laboratory of Infectious Respiratory Disease, Jinan, Shandong, China
Department of Lab Medicine, Shandong Public Health Clinical Center, Cheeloo College of Medicine, Shandong University, Jinan 250013, China

Corresponding authors.
E-mail addresses: zhangtbgroup@163.com (Y.-A. Zhang), wangmaoshui@gmail.com (M.-S. Wang)

Epidemiological characteristics of varicella before and after the implementation of two-dose vaccination schedule in Chaoyang District, Beijing, 2007–2019
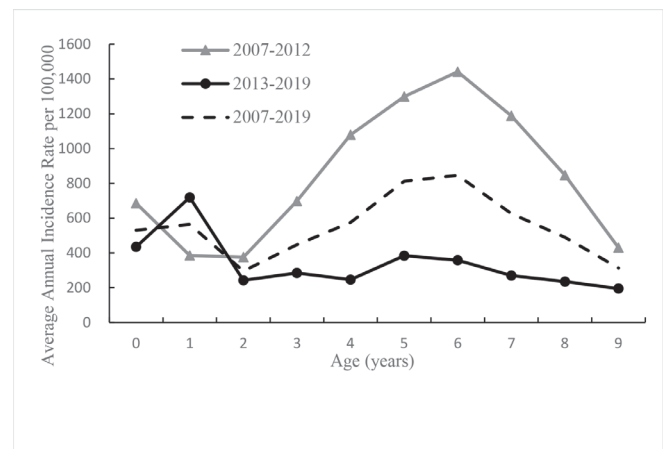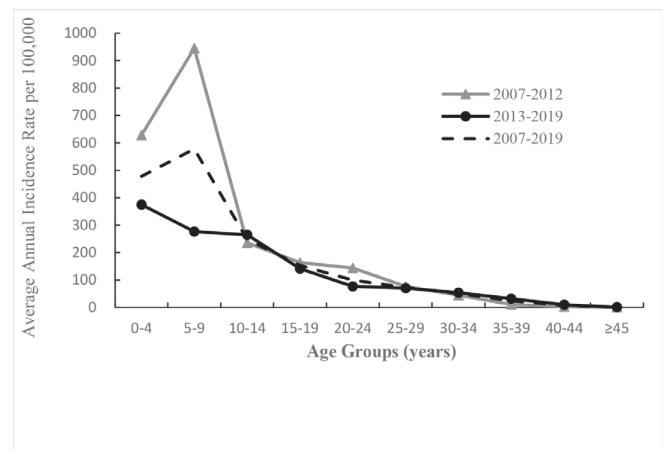
Dear editor,

We read with interest the paper by Quinn and colleagues[1] in this Journal. They concluded that the Australia's program has impacted on the burden of varicella disease, but vaccine effectiveness of single dose against varicella hospitalizations only moderate. In October 2012, Beijing center for disease control and prevention issued "the technical guideline of varicella vaccine uses in Beijing", recommending vaccinations schedule of two-dose (at 18 months and 4 years)[2]. In order to evaluate the impact of two-dose vaccination schedule on the incidence of varicella, we compared the epidemiological characteristics before and after implementation in Chaoyang District.

For surveillance purpose, varicella is defined as a clinically diagnosed illness with acute onset of a generalized vesicular rash excluding other causes. In February 2007, Beijing required varicella cases to be reported according to the requirements of Class C infectious diseases. Any clinical practitioners should report cases of varicella within 24 h through the National Notifiable Disease Reporting System (NNDRS). Epidemiological data and population data in this paper are collected from the NNDRS, with 2007–2012 as the pre-implementation period and 2013–2019 as the post-implementation period of the two-dose vaccination schedule.

During 2007–2019, a total of 34,122 cases of varicella were reported in Chaoyang District, Beijing, with an annual incidence of 53.91 per 100,000 populations to 108.12 per 100,000 populations, showing a decreasing trend. The average annual incidence rate before the implementation of two-dose vaccination schedule was 60.24 per 100,000 populations, which was 39.02% lower than that after the implementation of the 98.80 per 100,000 populations. Varicella occur year-round with peak months from May to June and from November to December. Compared with the pre-implementation levels, the average annual numbers of cases in May-June and November-December after implementation dropped by 42.62% and 34.41%, respectively.

Compared with the pro-implementation levels, the incidence of varicella in the age groups of 0–4,5–9 and 20–24 significantly reduced ($\chi 2$=82.473, $P < 0.001$;$\chi 2$=377.303, $P < 0.001$; $\chi 2$=71.672, $P < 0.001$), especially in the age group of 5–9, which was 276.59 per 100,000 populations, there was a decrease of 70.74% from 945.20 per 100,000 populations; while the age groups of 35–39,40–44 increased significantly($\chi 2$=25.451, $P < 0.001$;$\chi 2$=8.873, $P = 0.003$), and no statistical difference among the age groups of 11–14,15–19,25–29,30–34,45 and over (Fig. 1). Among children aged 0–9 years, the incidence rate of 1-year-old children increased from 385.07 per 100,000 populations before implementation to 719.53 per 100,000 populations after implementation, while it decreased significantly in other age groups($P < 0.01$) (Fig. 2). The median age of onset showed an upward trend year by year, from 8 years old in 2007 to 22 years old in 2019.

From the incidence data in Chaoyang District, it can be seen that the implementation of the 2-dose vaccination schedule further reduced the incidence of varicella. Firstly, the annual average reported incidence of varicella has declined marked. Secondly, the annual average number of cases in the peak months (May-June and November-December) dropped substantially. Thirdly, the incidence of varicella in the 0–4, 5–9 and 20–24 age groups decreased significantly, especially in the target age group (5–9 years) of the second dose of varicella vaccine.

The switching of vaccination schedule from one to two doses could further reduce the incidence of varicella, which was also confirmed by data from other regions or countries.[3-6] For countries or areas preparing to include varicella vaccine in their immunization programs, the WHO Position Paper[7] recommends that effective surveillance systems be established to assess the varicella burden prior to introduction and continued monitoring after in-

troduction. Beijing carried out varicella surveillance as early as five years before the implementation of the 2-dose schedule, which ensured that the impact of the 2-dose vaccination on the incidence of varicella could be assessed, thus providing experience for other regions and countries to develop varicella vaccination schedule. In addition, it should be noted that vaccination can significantly reduce the incidence of varicella but coverage must be maintained consistently at a certain level.[8,9]

After the implementation of the 2-dose vaccination schedule, the infection age tends to shift to the older age groups in Chaoyang District. Firstly, the median age of onset showed an upward trend year by year, from 8 years old in 2007 to 22 years old in 2019. Secondly, the incidences of 35–39 years and 40–44 years increased after implementation. It is thought that widespread childhood vaccination reduces risk of infection, leading to an increase in the average age of exposure to Varicella-Zoster Virus (VZV).[10] An upward shift in age of infection should be given attention, because adult patients with varicella have more severe symptoms, higher risk of death and complications compared to children.[7]

Another change in the epidemiology of VZV after implementation is that the incidence of 1-year-old children is significantly higher than before implementation. This was not observed in previous studies[3,4], because those studies analyzed age-specific data before and after implementation using the age interval of 3–5 years. It should be noted that the initial age for the first dose after implementation is 18 months by the technical guideline, while which before implementation is 12 months by the instructions of manufacturers. Further studies are needed to determine whether this change is associated with increased morbidity in the 1-year-old group. It also suggests that children should receive varicella vaccine in time to reduce the risk of infection.

To sum up, the implementation of the recommended guideline for two doses of varicella vaccine has led to a dramatic decline in varicella incidence in Chaoyang District, especially among the target group (5–9 years old) of the second dose. However, there are two noteworthy changes in the epidemiological characteristics after implementation, one is that the median age of varicella infection has shifted to adults, the other is that the incidence rate of 1-year-old children has increased.

Supplementary materials

Supplementary material associated with this article can be found, in the online version, at doi:10.1016/j.jinf.2021.07.035.

References

[1]. Quinn H.E., Gidding H.F., Marshall H.S., Booy R., Elliott E.J., Richmond P.. Varicella vaccine effectiveness over 10 years in Australia; moderate protection from 1-dose program. *J Infect* 2019;**78**:220–5 https://doi.org/. doi:10.1016/j.jinf.2018.11.009.
[2]. . Beijing center for disease control and prevention. the technical guideline of varicella vaccine uses in Beijing. *Chin J Prev Med* 2013;**47**:67–9 In Chinese.
[3]. Fu J., Jiang C., Wang J., Zhao F., Ma T., Shi R.. Epidemiology of varicella in Haidian district, Beijing, China-2007-2015. *Vaccine* 2017;**35**:2365–71 https://doi.org/. doi:10.1016/j.vaccine.2017.03.044.
[4]. Pan X., Ma R., Fang T., Dong H., Xu G.. Impact of a 2-dose varicella vaccination strategy on the incidence of varicella in Ningbo city. *Chin J Vaccines Immun* 2018;**24**:434–6 In Chinese.
[5]. Lopez A.S., Zhang J., Marin M.. Epidemiology of varicella during the 2-dose varicella vaccination program - United States, 2005-2014. *MMWR Morb Mortal Wkly Rep* 2016;**65**:902–5 https://doi.org/. doi:10.15585/mmwr.mm6534a4.
[6]. GarcíaCenoz M., Castilla J., Chamorro J., Martínez-Baz I., Martínez-Artola V., Irisarri F.. Impact of universal two-dose vaccination on varicella epidemiology in Navarre, Spain, 2006 to 2012. *Euro Surveill* 2013;**18**:20552 https://doi.org/. doi:10.2807/1560-7917.es2013.18.32.20552.
[7]. . Varicella and herpes zoster vaccines: WHO position paper, June 2014–Recommendations. *Vaccine* 2016;**34**:198–9 https://doi.org/. doi:10.1016/j.vaccine.2014.07.068.
[8]. Brisson M., Edmunds W.J., Gay N.J., Law B., De Serres G.. Modelling the impact of immunization on the epidemiology of varicella zoster virus. *Epidemiol Infect* 2000;**125**:651–69 https://doi.org/. doi:10.1017/s0950268800004714.
[9]. Gidding H.F., Brisson M., Macintyre C.R., Burgess M.A.. Modelling the impact of vaccination on the epidemiology of varicella zoster virus in Australia. *Aust N Z J Public Health* 2005;**29**:544–51. doi:10.1111/j.1467-842x.2005.tb00248.x.
[10]. Edmunds W.J., Brisson M.. The effect of vaccination on the epidemiology of varicella zoster virus. *J Infect* 2002;**44**:211–19 https://doi.org/. doi:10.1053/jinf.2002.0988.

Hongyu Wang[1]
Baotou Medical College, Inner Mongolia University of Science and Technology, Baotou, China
Chaoyang District Center for Disease Control and Prevention, Beijing, China

Fang Liu[1], Yang Cao, Nan Zhang
Chaoyang District Center for Disease Control and Prevention, Beijing, China

*Corresponding Author.
E-mail address:* liu1210@126.com (F. Liu)

[1] Both authors contributed equally to this work
Accepted 26 July 2021
Available online 29 July 2021

https://doi.org/10.1016/j.jinf.2021.07.035

Emergence of novel recombinant type 2 porcine reproductive and respiratory syndrome viruses with high pathogenicity for piglets in China

Dear editor:

Several studies in this journal reported genetic diversity of African swine fever virus (ASFV) genomes and suggested ASFV was a potential threat to unaffected countries in Asia.[1–3] Porcine reproductive and respiratory syndrome (PRRS), caused by porcine reproductive and respiratory syndrome virus (PRRSV), is another swine viral disease causing huge economic losses to the global swine industry.[4] PRRSV is an enveloped, positive-strand RNA virus under the family *Arteriviridae*. This virus is divided into major types, the North American type 2 and the European type 1, with VR-2332 and Lelystad as prototypical strains, respectively.[5] Emergence of novel PRRSV strains have caused many outbreaks of severe PRRS.[6] Since 2013, several PRRSV NADC30-like strains, sharing a unique discontinuous deletion of 131 aa in non-structural protein 2 (nsp2), have emerged in China and caused outbreaks.[7] In 2020, a novel PRRSV variant, with a 142aa deletion in nsp2, emerged in north China. Via this letter we report the unique genetic characteristics of this novel PRRSV variant and its pathogenicity for piglets.

During July to October 2020, severe outbreaks of PRRS with 100% morbidity and approximately 70% mortality were observed on different pig farms in Wuqing, Beichen, and Baodi districts of Tianjin, China. The infected nursery piglets showed high fever (41–42 °C) and respiratory disorders characterized by coughing, dyspnea, and tachypnea. Moreover, the above PRRS-infected swine farms showed a significant increase of secondary infections of bacterium, including *Haemophilus parasuis*, *Streptococcus suis*, *Mycoplasma hyopneumoniae*, etc.

Using real-time PCR tests, the serum samples collected in the detected swine farms in Wuqing districts of Tianjin was confirmed to be positive for PRRSV and negative for African swine fever virus (ASFV). Then the above serum samples were inoculated

into porcine alveolar macrophages (PAMs) cells as described previously for virus isolation.[8] The strain, designated TJwq2020, was subsequently isolated and the full-length genomic sequence was determined. The genome of TJwq2020 has a size of 14.987 kg-bases (excluding the poly (A) tail), and shares 84.8 and 60.7% sequence identity with VR2332 and LV, respectively. This indicates that TJwq2020 belongs to the type 2 PRRSV. The amino acid alignment of the Nsp2 of TJwp2020 showed that TJwq2020 had a new deletion pattern of "111-aa+11-aa+1-aa+19-aa" in its Nsp2-coding region (nt322– nt432, nt466–nt476, nt483, nt504–nt522) when compared with the sequence of VR-2332. This deletion of the nsp2 of TJwq2020 is a novel deletion compared to that of previous PRRSV isolates.

To establish the genetic relationships between TJwq2020 and other PRRSV strains, phylogenetic trees were constructed using the neighbor-joining method.[9] The results showed that TJwq2020 is clustered as lineage 1 (Chsx1401-/NADC30- /MN184-like) based on the full-length genome, but clustered as lineage 8 (JXA1- /HB-1/CH-1a-like) based on 5′UTR and Nsp4–8. These results indicate that mosaic recombination events may have occurred in the genome of the TJwq2020 isolate. To test this hypothesis, a software approach was used to detect possible recombination events within TJwq2020.

The similarity comparisons were performed by using Sim-Plotv3.5.1 software to identify possible recombination events.[10] Based on a set of complete genome sequences of various PRRSV strains, including lineage 1 strains (Chsx1401, NADC30, MN184C), and lineage 8 strains (JXA1, HB-1, CH-1a), the SimPlot graph clearly showed that TJwq2020 is closer to NADC30 than to any other strains. However, there were 2 narrow zones showing disproportionately low levels of similarity between the 2 strains compared to other regions (Fig. 1). Notably, the 2 narrow zones of TJwq2020 had high levels of similarity with HB-1 (a lineage 8.1 strain, isolated in Hebei, China in 2002). These results indicate that TJwq2020 is a recombinant possibly between parental-like strains NADC30 and HB-1. The recombination mechanism was further analyzed by Bootscan.

Three potential recombination breakpoints were identified, which were located in Nsp1 (nt728), Nsp3 (nt5337) and Nsp9 (nt7992). The breakpoints separated the genome into four regions, where region A (nt1-nt728) and region C (nt5337-nt7992) were closely related to lineage 8 (JXA1-/HB-1-/CH-1a-like) strain, whereas region B (nt729-nt5336) and region D (nt7993-nt14987) were closely related to lineage 1 (CHsx1401-/NADC30-/MN184-like). This evidence further supported the hypothesis that TJwq2020 is a natural recombinant between NADC30 (lineage1 strain) and HB-1(lineage 8 strain).

To determine the pathogenicity of TJqw2020, ten 4-week-old piglets were randomly divided into two groups ($n = 5$). The piglets in challenge group ($n = 5$) were inoculated intramuscularly (1 ml) and intranasally (2 ml) with TJqw2020-F3 ($2 \times 10^{4.0}$ TCID$_{50}$ in 3 ml per pig). The negative control group piglets were mock infected with 3 ml of DMEM. The inocula were free of bacteria, Mycoplasma, ASFV, CSFV, PCV2, and SIV. The rectal temperature and clinical signs of the piglets were daily recorded. Serum samples were collected on 0, 3, 5, 7, 10, 14 and 21 days post inoculation (dpi) for PRRSV N protein antibody detection (IDEXX, USA, and the cut off value of S/P was 0.4). The piglets died or were euthanized on 21 dpi, and were necropsied for histopathologic examinations.

The rectal temperature of piglets in the TJwq2020-inoculated group exhibited short duration of fever (40.2 °C) at 1–3 dpi and then stayed normal for consecutive 5 days. However, the TJwq2020-inoculated piglets showed high and continuous fever from 9 dpi to 14 dpi (Fig. 2A) with severe symptoms of disease progress, such as cough, anorexia, and red discoloration of the body. The antibody was detected in 40.0% (2/5) of TJwq2020-inoculated piglets at 3dpi with lower antibody levels (compared to antibody of inoculated piglets at 10 dpi and 14 dpi) and converted antibody negative at 5 dpi and 7 dpi. On 10 dpi, 100% (5/5) of the TJwq2020- inoculated piglets' serum samples were tested antibody positive (Fig. 2B). Severe interstitial pneumonia with extensive and marked pulmonary edema, hemorrhage and consolidation were observed in TJwq2020-inoculated piglets, and fibrinous pneumonia and pericarditis were also found at necropsy of dead piglets (data not shown). 100% (5/5) piglets died within 14 days after the TJwq2020 inoculation (Fig. 2C). No obvious clinical signs were observed in the control group during the entire experiment period.

In summary, we isolated TJwq2020, a novel PRRSV variant with a unique continuous deletion of 142aa in Nsp2 in China. We demonstrated that this TJwq2020 is a natural recombinant between NADC30 (lineage1 strain) and HB-1 (lineage 8 strain). Exper-
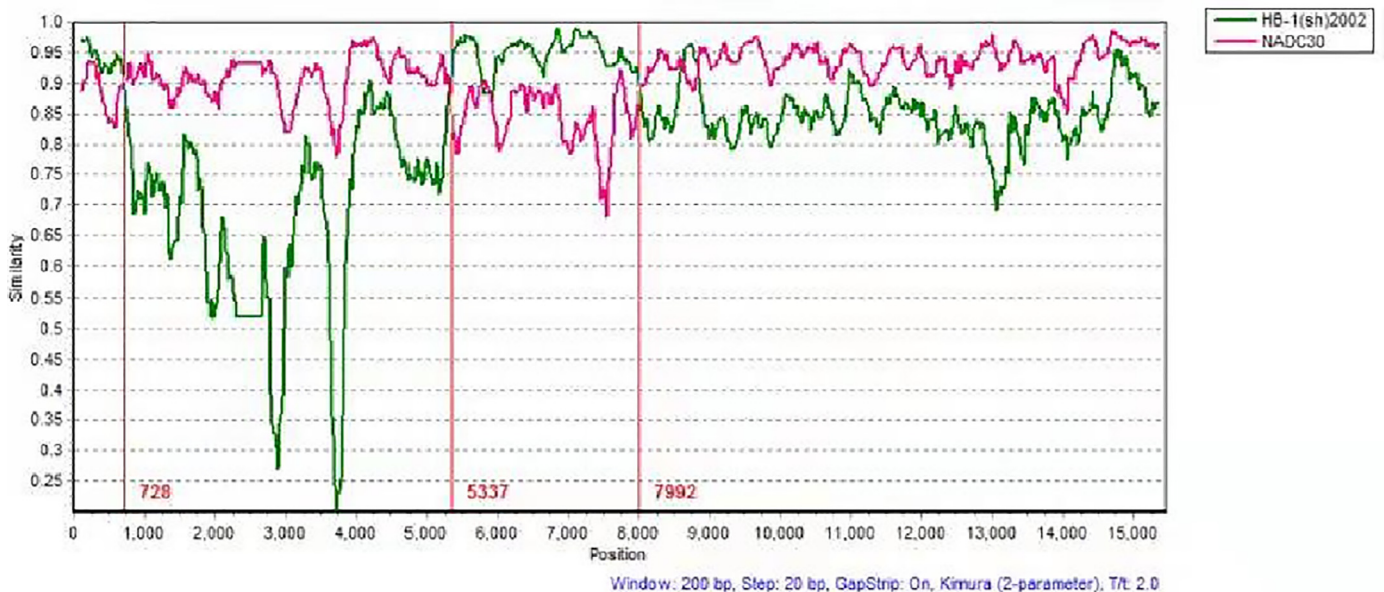
Fig. 1. Recombination event analyses of the TJwq2020 strain of porcine reproductive and respiratory syndrome virus (PRRSV). Similarity plot analysis using TJwq2020 as query sequence. Analysis made use of a sliding window of 200 bases and a step size of 20 bases. The y-axis shows the percentage similarity between the selected PRRSV sequences and the query sequence. The other comparisons are not shown for clarity.
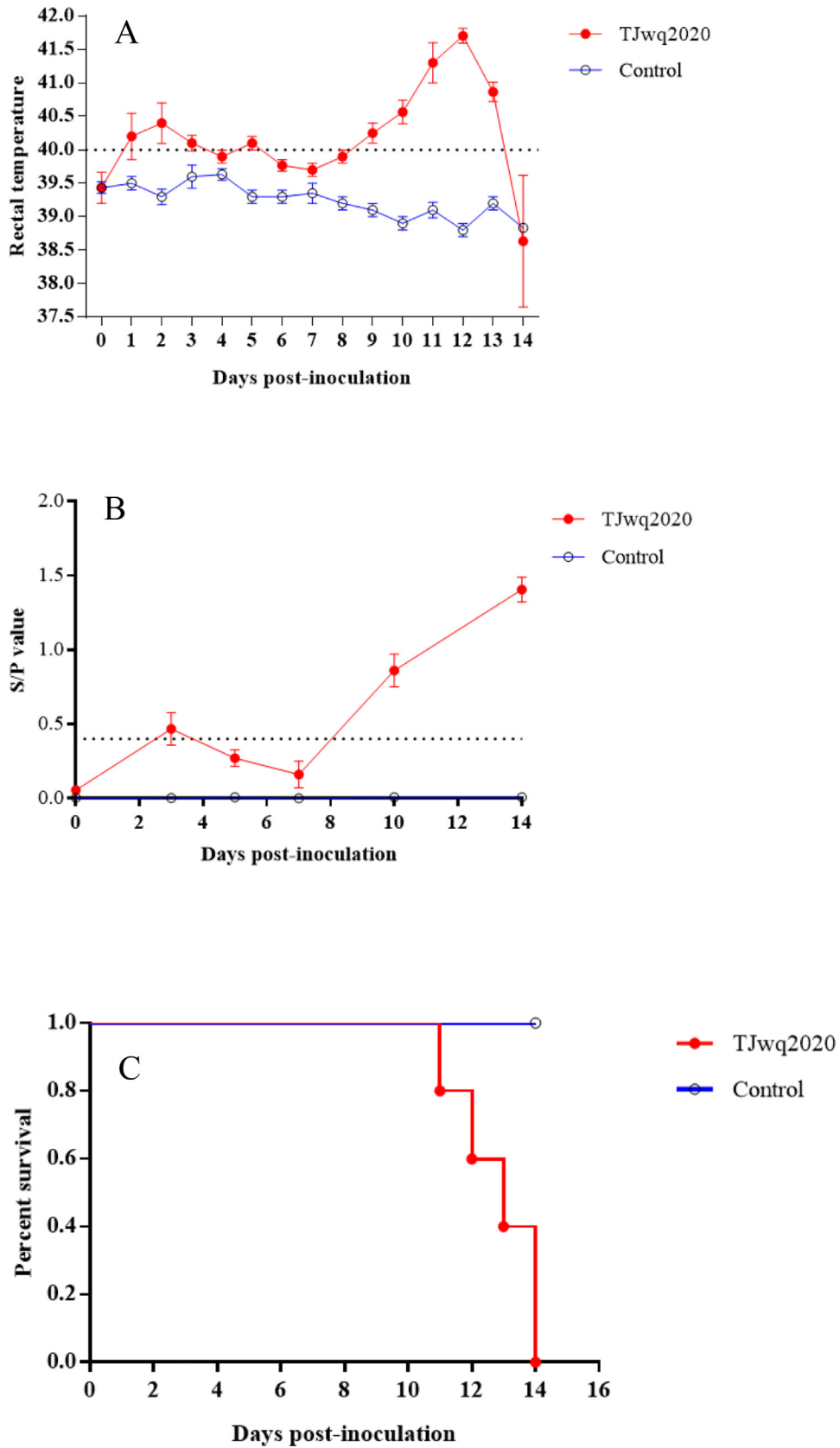
Fig. 2. The pathogenicity of TJwq2020. Ten 4-week-old piglets ($n = 5$) free of PRRSV were inoculated intramuscularly (1 ml) and intranasally (2 ml) with TJqw2020-F3 ($2 \times 10^{4.0}$ TCID$_{50}$ in 3 ml per pig). Mean rectal temperature (A), antibody level (B), and survival rate (C) of each group were recorded for 14 dpi.

iments in piglets demonstrated that TJqw2020 is a highly virulent strain. Our study suggests that recombination might be responsible for the varying pathogenicity of type 2 PRRSV strains, and highlights the importance of monitoring highly virulent recombinant PRRSV strains.

Declaration of Competing Interest

The authors have declared that no conflicts of interest.

Funding

References

1. Ye C., Wu X.P., Chen T.T., Huang Q.Y., Fang R.D., An T.Q.. The updated analysis of African swine fever virus genomes: two novel genotypes are identified. *J Infect* 2020;**80**(2):232–54. doi:10.1016/j.jinf.2019.10.013.
2. Li X.B., Xiao K.P., Zhang Z.P., Yang J.J., Wang R.C., Shen X.J., et al. The recombination hot spots and genetic diversity of the genomes of African swine fever viruses. *J Infect* 2020;**80**(1):121–42. doi:10.1016/j.jinf.2019.08.007.
3. Lu G., Pan J.L., Zhang G.H.. African swine fever virus in Asia: its rapid spread and potential threat to unaffected countries. *J Infect* 2020;**80**(3):350–71. doi:10.1016/j.jinf.2019.11.011.
4. Eric J.N., James B.K., Colin D.J., John W.M., Eric J.B., Ann H.S., et al. Assessment of the economic impact of porcine reproductive and respiratory syndrome on swine production in the United States. *J Am Vet Med Assoc* 2005;**227**(3):385–92. doi:10.2460/javma.2005.227.385.
5. Lunney J.K., Fang Y., Ladinig A., Chen N., Li Y., Rowland R.R., et al. Porcine reproductive and respiratory syndrome virus (PRRSV): pathogenesis and interaction with the immune system. *Annu Rev Anim Biosci* 2016;**4**:129–54. doi:10.1146/annurev-animal-022114-111025.
6. Tian K., Yu X., Zhao T., Feng Y., Cao Z., Wang C., et al. Emergence of fatal PRRSV variants: unparalleled outbreaks of a typical PRRS in China and molecular dissection of the unique hallmark. *PLoS ONE* 2007;**2**(6):e526. doi:10.1371/journal.pone.0000526.
7. Zhou L., Wang Z.C., Ding Y.P., Ge X.N., Guo X., Yang H.C.. NADC30-like strain of porcine reproductive and respiratory syndrome virus, China. *Emerg Infect Dis* 2015;**21**(12):2256–7. doi:10.3201/eid2112.150360.
8. Zhang H., Guo X., Ge X., Chen Y., Sun Q., Yang H.. Changes in the cellular proteins of pulmonary alveolar macrophage infected with porcine reproductive and respiratory syndrome virus by proteomics analysis. *J Proteome Res* 2009;**8**(6):3091–7. doi:10.1021/pr900002f.
9. Zhao K., Ye C., Chang X.B., Jiang C.G., Wang S.J., Cai X.H., et al. Importation and recombination are responsible for the latest emergence of highly pathogenic porcine reproductive and respiratory syndrome virus in China. *J Virol* 2015;**89**(20):10712–16. doi:10.1128/JVI.01446-15.
10. Ramos N., Mirazo S., Castro G., Arbiza J.. Molecular analysis of porcine circovirus Type2 strains from Uruguay: evidence for natural occurring recombination. *Infect Genet Evol* 2013;**19**:23–31. doi:10.1016/j.meegid.2013.06.017.

Ying-Feng Sun, Jing Yang, Ye Liu, Wen-Zhong Li, Xiao-Xue Yu, Liu-An Li*

Tianjin Key Laboratory of Agricultural Animal Breeding and Healthy Husbandry, College of Animal Science and Veterinary Medicine, Tianjin Agricultural University, Tianjin 300384, China

Hai Yu**

Shanghai Veterinary Research Institute, Chinese Academy of Agricultural Sciences, No.518, Ziyue Roa, Minhang District, Shanghai 200241, China
Jiangsu Co-innovation Center for Prevention and Control of Important Animal, Infectious Diseases and Zoonoses, Yangzhou 225009, China

*Corresponding author**Corresponding author at: Shanghai Veterinary Research Institute, Chinese Academy of Agricultural Sciences, No.518, Ziyue Road, Minhang District, Shanghai 200241, China.*
E-mail addresses: anliuli2003@163.com (L.-A. Li), haiyu_008@126.com (H. Yu)

Infection-enhancing anti-SARS-CoV-2 antibodies recognize both the original Wuhan/D614G strain and Delta variants. A potential risk for mass vaccination?

Dear editor,

The aim of the present study was to evaluate the recognition of SARS-CoV-2 Delta variants by infection enhancing antibodies directed against the NTD. The antibody studied is 1052 (pdb file #7LAB) which has been isolated from a symptomatic Covid-19 patient[1]. Molecular modeling simulations were performed as previously described[2]. Two currently circulating Delta variants were investigated, with the following mutational patterns in the NTD :

- G142D/E154K (B.1.617.1)
- T19R/E156G/del157/del158/A222V (B.1.617.2)

Each mutational pattern was introduced in the original Wuhan/D614G strain, submitted to energy minimization, and then tested for antibody binding. The energy of interaction (ΔG) of the reference pdb file #7LAB (Wuhan/D614G strain) in the NTD region was estimated to -229 kJ/mol^{-1}. In the case of Delta variants, the energy of interaction was raised to -272 kJ.mol^{-1} (B.1.617.1) and -246 kJ.mol^{-1} (B.1.617.2). Thus, these infection enhancing antibodies not only still recognize Delta variants but even display a higher affinity for those variants than for the original SARS-CoV-2 strain.

The global structure of the trimeric spike of the B.1.617.1 variant in the cell-facing view is shown in **Fig. 1A**. As expected, the facilitating antibody bound to the NTD (in green) is located behind
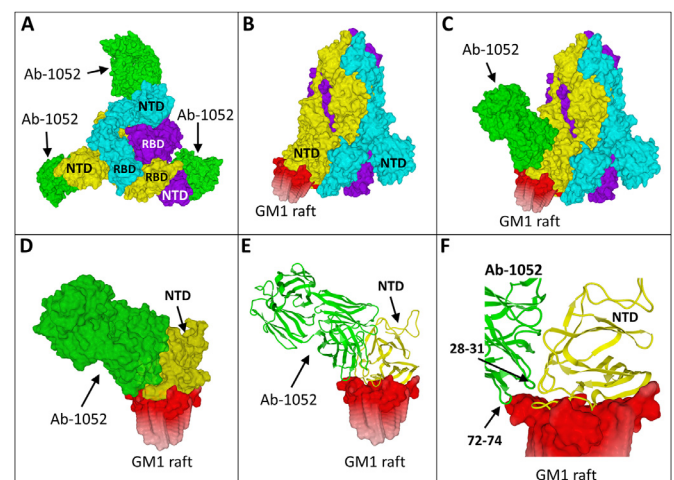
Fig. 1. Infection enhancing antibodies recognize the NTD of Delta variants. **A.** Molecular model of the Delta B.1.617.1 spike trimer as viewed from the host cell surface (chains A, B and C in cyan, yellow and purple, respectively), with the NTD and RBD of each chain indicated. The 1052 antibody is in green. **B.** Spike trimer with the B subunit bound to a lipid raft (with 6 ganglioside GM1 molecules). **C.** Trimolecular [spike-antibody-raft] complex. **D.** Focus on the NTD-antibody complex bound to the lipid raft. **E.** Secondary structures of the NTD (yellow) and the antibody (green) bound to lipid raft gangliosides. **F.** The 1052 antibody clamps the NTD and the edge of the lipid raft.

Fig. 2. Neutralization vs ADE balance according to SARS-CoV-2 strains.

the contact surface so that it does not interfere with virus-cell attachment. Indeed, a preformed antibody-NTD complex could perfectly bind to the host cell membrane. The interaction between the NTD and a lipid raft is shown in **Fig. 1B**, and a whole raft-spike-antibody complex in **Fig. 1C**. Interestingly, a small part of the antibody was found to interact with the lipid raft, as further illustrated in **Figs. 1D-E**. More precisely, two distinct loo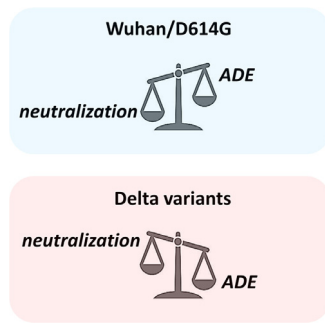ps of the heavy chain of the antibody encompassing amino acid residues 28–31 and 72–74, stabilize the complex through a direct interaction with the edge of the raft (**Fig. 1F**). Overall, the energy of interaction of the NTD-raft complex was raised from -399 kJ.mol^{-1} in absence of the antibody to -457 kJ.mol^{-1} with the antibody. By clamping the NTD and the lipid raft, the antibody reinforces the attachment of the spike protein to the cell surface and thus facilitates the conformational change of the RBD which is the next step of the virus infection process[2].

This notion of a dual NTD-raft recognition by an infection enhancing antibody may represent a new type of ADE that could be operative with other viruses. Incidentally, our data provide a mechanistic explanation of the FcR-independent enhancement of infection induced by anti-NTD antibodies[1]. The model we propose, which links for the first time lipid rafts to ADE of SARS-CoV-2, is in line with previous data showing that intact lipid rafts are required for ADE of dengue virus infection[3].

Neutralizing antibodies directed against the NTD have also been detected in Covid-19 patients[4-5]. The 4A8 antibody is a major representant of such antibodies[5]. The epitope recognized by this antibody on the flat NTD surface is dramatically affected in the NTD of Delta variants[2], suggesting a significant loss of activity in vaccinated people exposed to Delta variants. More generally, it can be reasonably assumed that the balance between neutralizing and facilitating antibodies may greatly differ according to the virus strain (**Fig. 2**).

Current Covid-19 vaccines (either mRNA or viral vectors) are based on the original Wuhan spike sequence. Inasmuch as neutralizing antibodies overwhelm facilitating antibodies, ADE is not a concern. However, the emergence of SARS-CoV-2 variants may tip the scales in favor of infection enhancement. Our structural and modeling data suggest that it might be indeed the case for Delta variants.

In conclusion, ADE may occur in people receiving vaccines based on the original Wuhan strain spike sequence (either mRNA or viral vectors) and then exposed to a Delta variant. Although this potential risk has been cleverly anticipated before the massive use of Covid-19 vaccines[6], the ability of SARS-CoV-2 antibodies to mediate infection enhancement in vivo has never been formally demonstrated. However, although the results obtained so far have been rather reassuring[1], to the best of our knowledge ADE of Delta variants has not been specifically assessed. Since our data indicate that Delta variants are especially well recognized by infection enhancing antibodies targeting the NTD, the possibility of ADE should

be further investigated as it may represent a potential risk for mass vaccination during the current Delta variant pandemic. In this respect, second generation vaccines[7] with spike protein formulations lacking structurally-conserved ADE-related epitopes should be considered.

References

1. Li D., et al. In vitro and in vivo functions of SARS-CoV-2 infection-enhancing and neutralizing antibodies. *Cell* 2021;**184**:4203–19.
2. Fantini J., Yahi N., Azzaz F., Chahinian H.. Structural dynamics of SARS-CoV-2 variants: a health monitoring strategy for anticipating Covid-19 outbreaks. *J Infect* 2021;**83**:197–206.
3. Puerta-Guardo H., Mosso C., Medina F., Liprandi F., Ludert J.E., del Angel R.M.. Antibody-dependent enhancement of dengue virus infection in U937 cells requires cholesterol-rich membrane microdomains. *J Gen Virol* 2010;**91**:394–403.
4. Chi X., et al. A neutralizing human antibody binds to the N-terminal domain of the Spike protein of SARS-CoV-2. *Science* 2020;**369**:650–5.
5. Liu L., et al. Potent neutralizing antibodies against multiple epitopes on SARS–CoV-2 spike. *Nature* 2020;**584**:450–6.
6. Iwasaki A., Yang Y.. The potential danger of suboptimal antibody responses in COVID-19. *Nat Rev Immunol* 2020;**20**:339–41.
7. Fantini J., Chahinian H., Yahi N.. Leveraging coronavirus binding to gangliosides for innovative vaccine and therapeutic strategies against COVID-19. *Biochem Biophys Res Commun* 2021;**538**:132–6.

Nouara Yahi
Henri Chahinian
Jacques Fantini
INSERM UMR_S 1072, Aix-Marseille Université, 13015 Marseille, France

Changes in the pathogenic spectrum of acute respiratory tract infections during the COVID-19 epidemic in Beijing, China: A large-scale active surveillance study

Dear editor,

Poole and colleagues demonstrated the impact of coronavirus disease 2019 (COVID-19) pandemic on the epidemiology of general respiratory viruses.[1] The prevalence of non-SARS-CoV-2 viruses during the COVID-19 epidemic has not been wildly reported in China. We conducted to analyze the surveillance data of respiratory pathogens to explore the impact of public health measures against COVID-19 on the prevalence of non-SARS-CoV-2 pathogens in China.

Among 41,630 acute respiratory tract infections (ARTIs) between 01/02/2015 and 31/01/2021 in 35 hospitals from the Respiratory Pathogen Surveillance System (detailed in Supplemental materials), 37,490 (25,658 adults and 11,832 children) occurred before the COVID-19 epidemic (01/02/2015–31/01/2020), and 4140 (3379 adults and 761 children) occurred during the COVID-19 epidemic (01/02/2020–31/01/2021) (Fig. 1A-B).

All 41,630 cases were tested for 11 respiratory tract pathogens and 13,630 (32.74%, 95% CI 32.29% to 33.19%) had at least one positive result. Before the COVID-19 epidemic, the most common pathogen among the positive cases was influenza virus (IFV), followed by *mycoplasma pneumoniae* (MP), human parainfluenza virus (HPIV), human rhinovirus (HRV), enterovirus (EV), respiratory syncytial virus (RSV), seasonal human coronavirus (HCoV), human
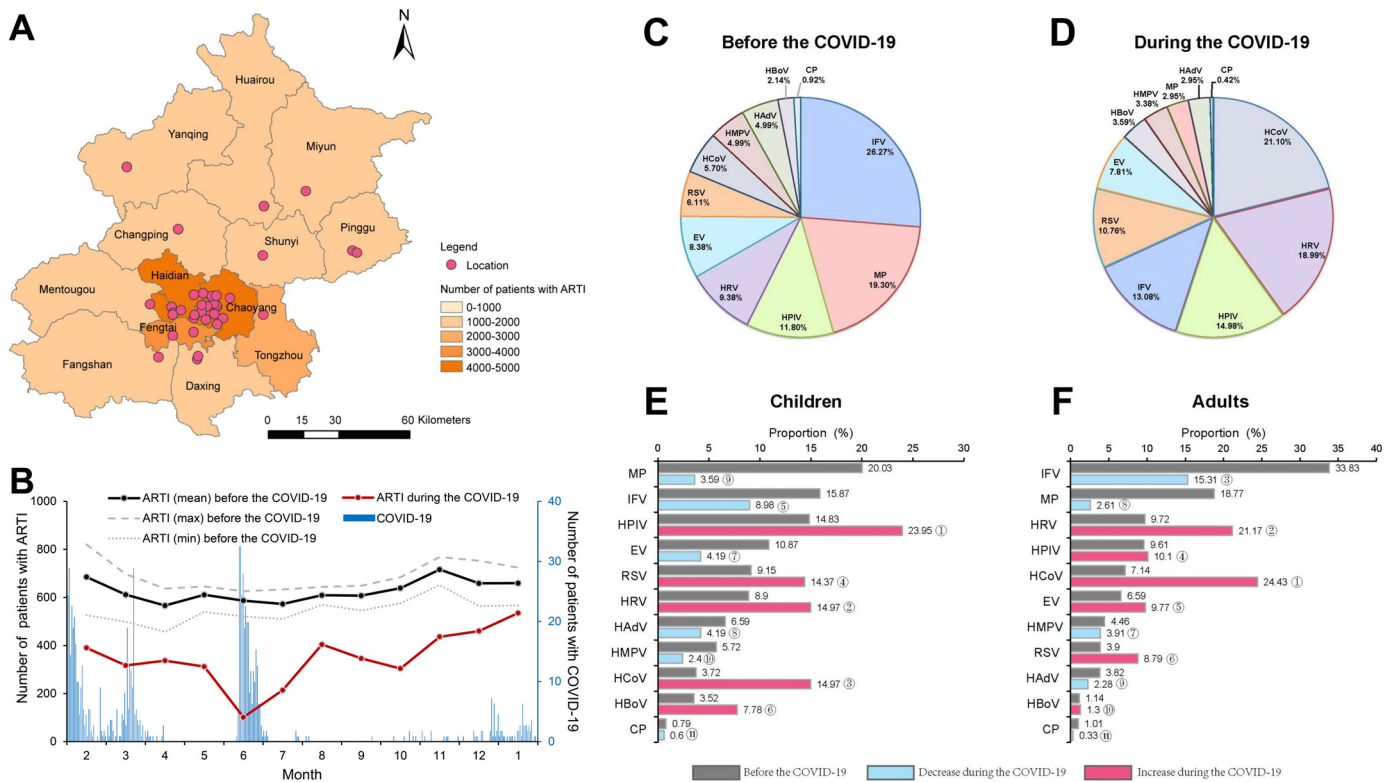
Fig. 1. Spatial and temporal distribution of the samples and pathogenic spectrum from acute respiratory tract infections before the COVID-19 and during the COVID-19.

A, the distribution of 35 sentinel hospitals. The red dot represents the location of the hospital.

B, the monthly distribution of samples. The red line represents the number of samples from ARTI during the epidemic of the COVID-19. The black line represents the mean number of samples from ARTI before the epidemic of the COVID-19. The long dash gray line represents the max number of samples from ARTI before the epidemic of the COVID-19. The dot dash gray line represents the min number of samples from ARTI before the epidemic of the COVID-19. The blue column represents the number of the COVID-19 patients using the right vertical axis.

C, the pie chart for pathogenic spectrum of acute respiratory tract infections before the COVID-19; D, the pie chart for pathogenic spectrum of acute respiratory tract infections during the COVID-19; E, the column chart for pathogenic spectrum of acute respiratory tract infections for the children; F, the column chart for pathogenic spectrum of acute respiratory tract infections for the adults.

E-F, the gray column represents the proportion of the pathogen before the COVID-19; the blue column represents the proportion of the pathogen during the COVID-19, which decreased compared to that before the COVID-19; the red column represents the proportion of the pathogen during the COVID-19, which increased compared to that before the COVID-19.

The period between 1 February 2015 and 31 January 2020 for the control was as before the COVID-19 and the period between 1 February 2020 and 31 January 2021 was as during the COVID-19. COVID-19, coronavirus disease 2019.

metapneumovirus (HMPV), human adenovirus (HAdV), human bocavirus (HBoV) and *chlamydia pneumoniae* (CP), which changed to seasonal HCoV, followed by HRV, HPIV, IFV, RSV, EV, HBoV, HMPV, MP, HAdV and CP during the COVID-19 epidemic (Fig. 1C-F and Table S1-S3). SARS-CoV-2 was not detected. For children, the top five pathogens were MP, IFV, HPIV, EV and RSV before the COVID-19 epidemic, changing to HPIV, seasonal HCoV, HRV, RSV and IFV. For adults, the top five pathogens were IFV, MP, HRV, HPIV and seasonal HCoV before the COVID-19 epidemic, changing to seansonal HCoV, HRV, IFV HPIV and EV. All the other pathogens had distinct increases in proportions except for IFV.

Before the COVID-19 epidemic, 12,058 (32.16%, 95% CI 31.69% to 32.64%) were positive for at least one pathogen, which significantly dropped to 10.97% (95% CI 10.03% to 11.96%) during the COVID-19 epidemic (*P*<0.001, Fig. 2A and Table S4). The positive rates of the top five pathogens were IFV (9.22%), MP (6.77%), HPIV (4.14%), HRV (3.29%) and EV (2.94%) before the COVID-19 epidemic and seasonal HCoV (2.42%), HRV (2.17%), HPIV (1.71%), IFV (1.50%) and RSV (1.23%) during the COVID-19 epidemic. A similar trend was observed in children (from 41.92% to 20.76%, *P*<0.001) and in adults (from 27.66% to 8.76%, *P*<0.001).

Among all the pathogens, only seasonal HCoV had 20.74% increase in the positive rate, from 2.00% to 2.42% (*P* = 0.073). The other 10 pathogens had significant decreases in their positive rates

(all *P*<0.05). IFV had the largest difference (−7.72%, 95% CI −8.19% to −7.25%) in the positive rate decreasing by 83.75% (Fig. 2B).

In children, a significant increase in seasonal HCoV was observed from 1.74% to 3.29% (*P* = 0.002, Fig. 2A,C and Table S5). The positive rates of the top five pathogens were MP (9.37%), IFV (7.43%), HPIV (6.94%), EV (5.09%) and RSV (4.28%) before the COVID-19 epidemic and HPIV (5.26%), seasonal HCoV (3.29%), HRV (3.29%), RSV (3.15%) and IFV (1.97%) during the COVID-19 epidemic. The other nine pathogens showed decreased positive rates but significant for IFV, MP, EV, HMPV and HAdV (Fig. 2C).

In adults, seasonal HCoV slightly increased during the COVID-19 epidemic (*P* = 0.710, Fig. 2A and Table S6). The positive rates of the other nine pathogens significantly decreased except for RSV. The positive rates of the top five pathogens were IFV (10.04%), MP (5.57%), HRV (2.89%), HPIV (2.85%) and seasonal HCoV (2.12%) before the COVID-19 epidemic and seasonal HCoV (2.22%), HRV (1.92%), IFV (1.39%), HPIV (0.92%) and EV (0.89%) during the COVID-19 epidemic. IFV had the largest difference in the positive rate, followed by MP and HPIV (Fig. 2D).

After on 24/01/2020 in Beijing, the overall positive rates of all pathogens changed according to the implementation of different levels of PHER (Fig. 2E-P). The positive rates sharply decreased due to the outbreak of COVID-19 in the Xinfadi Market and in Shunyi District, Beijing. These results indicated the prevalence of
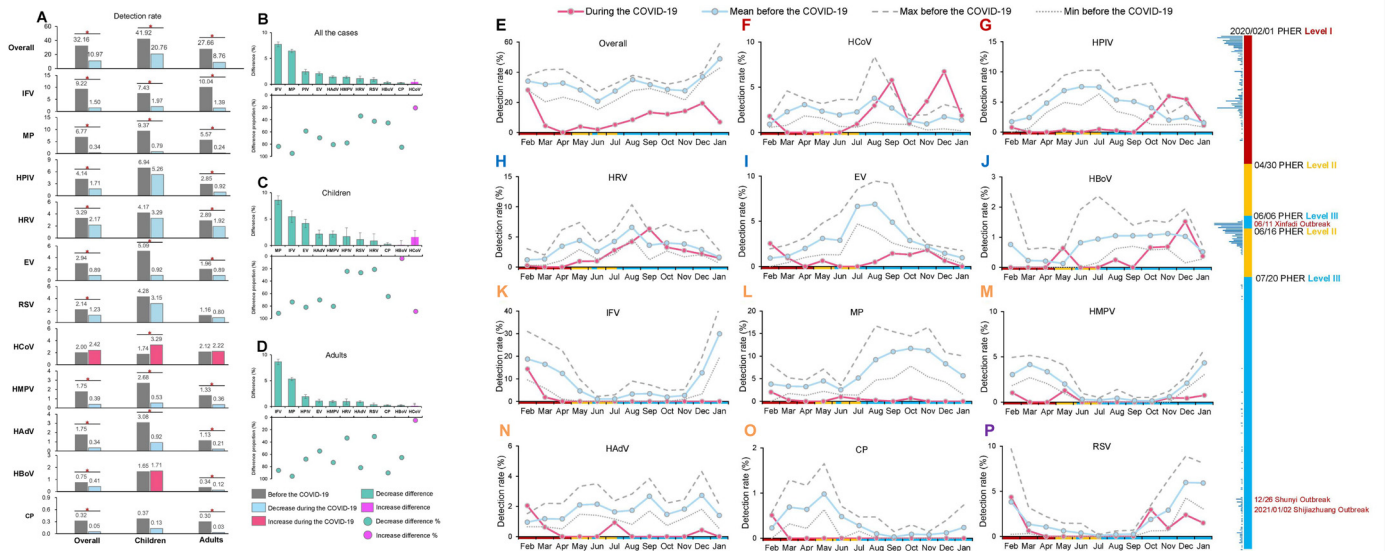
Fig. 2. The positive rate and dynamic profiles of the pathogens from acute respiratory tract infection before and during the COVID-19.

A, the positive rate of the pathogens as a whole and in the children and in the adults; the star means the significant difference between the positive rates before and during the COVID-19 by chi square test; The gray column represents the proportion of the pathogen before the COVID-19; the blue column represents the proportion of the pathogen during the COVID-19, which decreased compared to that before the COVID-19; the red column represents the proportion of the pathogen during the COVID-19, which increased compared to that before the COVID-19;

B, the difference (upper half part) and difference proportion (lower half part) between the positive rates before and during the COVID-19 as a whole;

C, the difference (upper half part) and difference proportion (lower half part) between the positive rates before and during the COVID-19 in the children;

D, the difference (upper half part) and difference proportion (lower half part) between the positive rates before and during the COVID-19 in the adults;

B-D, the green column/dot represents the decrease difference/difference proportion; the purple column/dot represents the increase difference/difference proportion; The difference of positive rates was defined as the positive rate during the COVID-19 minus the positive rate before the COVID-19. The difference proportion (%) was defined as the difference of positive rate (%) divided by the detection rate before the COVID-19.

E, overall; F, seasonal HCoV; G, HPIV; H, HRV; I, EV; J, HBoV; K, IFV; L, MP; M, HMPV; N, HAdV; O, CP; P, RSV. The red line represents the positive rate during the epidemic of the COVID-19. The blue line represents the positive rate before the epidemic of the COVID-19. The long dash gray line represents the max positive rate before the epidemic of the COVID-19. The dot dash gray line represents the min positive rate before the epidemic of the COVID-19. The right multi-colored strip represents the time line of the PHER in Beijing during from 1 February 2020 to 31 January 2021. The red part represents the PHER Level I; the yellow part represents the PHER Level II; the light blue part represents the PHER Level III. PHER, public health emerging response. The dark blue column represents the number of the COVID-19 patients in Beijing.

---

pathogens was closely related to public health measures against COVID-19.

Four groups were classified according to the dynamic trend of the positive rate of each pathogen. The positive rates of seasonal HCoV and HPIV were lower in the early stage of the COVID-19 epidemic and increased in the late stage, even exceeding the previous peak. For HRV, EV and HBoV, the positive rates returned to their previous levels in the late stage of the COVID-19 epidemic. The positive rates decreased to lower levels and remained until January 2021 for IFV, MP, HMPV, HAdV and CP. IFV was only detected in February and March 2020. COVID-19 had a relatively smaller effect on the positive rate of RSV compared to other pathogens.

Public health measures against COVID-19 and people's daily behavior changed potentially affected the prevalence of other respiratory pathogens.[2-6] The decrease of IFV is closely related to influenza vaccination as well as the public health measures. More influenza vaccinations may have effectively reduced the spread of IFV. The COVID-19 epidemic and the corresponding protective measures have changed people's medical behavior, with significant decreases in non-COVID-19 inpatient and outpatient visits.

Seasonal HCoV became the first pathogen in ARTIs during the COVID-19 epidemic. Anton et al. reported that the detection rates of HCoV and HPIV increased after the H1N1 epidemic in Catalonia, Spain.[7] Four seasonal HCoVs showed biennial incidence peaks in winter with alternating peak seasons for 229E and NL63, and OC43 and HKU1. Studies showed a biennial trend on the peak prevalence of seasonal HCoV in Beijing.[8,9] Therefore, the incidence of seasonal HCoV may have peaked in 2020/2021, which may have been higher without no public measures for COVID-19. This suggests that we need to further strengthen the monitoring of HCoV in the future

to prevent a co-epidemic of seasonal HCoV and SARS-CoV-2, especially when control measures for COVID-19 become normalized.

In general, public health measures against COVID-19 substantially reduced the prevalence of other respiratory pathogens. IFV decreased from the first to the fourth during the COVID-19 epidemic. Seasonal HCoV, which became the first pathogen of ARTIs, should be strengthened to control to prevent co-circulation with SARS-CoV-2.

These findings indicated the additional benefits of the public health measures implemented for COVID-19 in reducing the spread of other respiratory diseases.

Notes

Supplementary materials

Supplementary material associated with this article can be found, in the online version, at doi:10.1016/j.jinf.2021.08.013.

References

1. Poole S., Brendish N.J., Clark T.W.. SARS-CoV-2 has displaced other seasonal respiratory viruses: results from a prospective cohort study. *J Infect* Dec 2020;**81**(6):966–72 PubMed PMID: 33207254. Pubmed Central PMCID: PMC7666810. Epub 2020/11/19.
2. Zhang N., Jia W., Lei H., Wang P., Zhao P., Guo Y., et al. Effects of human behaviour changes during the COVID-19 pandemic on influenza spread in Hong Kong. *Clin Infect Dis* 2020 Dec 4 PubMed PMID: 33277643. Pubmed Central PMCID: PMC7799278. Epub 2020/12/06.
3. Soo R.J.J., Chiew C.J., Ma S., Pung R., Lee V.. Decreased Influenza Incidence under COVID-19 Control Measures, Singapore. *Emerg Infect Dis* Aug 2020;**26**(8):1933–5 PubMed PMID: 32339092. Pubmed Central PMCID: PMC7392467. Epub 2020/04/28.
4. Kuitunen I., Artama M., Makela L., Backman K., Heiskanen-Kosma T., Renko M.. Effect of Social Distancing Due to the COVID-19 Pandemic on the Incidence of Viral Respiratory Tract Infections in Children in Finland During Early 2020. *Pediatr Infect Dis J* Dec 2020;**39**(12):e423–e4e7 PubMed PMID: 32773660. Epub 2020/08/11.
5. Olsen S.J., Azziz-Baumgartner E., Budd A.P., Brammer L., Sullivan S., Pineda R.F., et al. Decreased Influenza Activity During the COVID-19 Pandemic - United States, Australia, Chile, and South Africa, 2020. *MMWR Morb Mortal Wkly Rep* 2020 Sep 18;**69**(37):1305–9 PubMed PMID: 32941415. Pubmed Central PMCID: PMC7498167 Journal Editors form for disclosure of potential conflicts of interest. Cheryl Cohen reports grants from Sanofi Pasteur and non-financial support from Parexel during the conduct of the study. No other potential conflicts of interest were disclosed. Epub 2020/09/18.
6. Sunagawa S., Iha Y., Kinjo T., Nakamura K., Fujita J.. Disappearance of summer influenza in the Okinawa prefecture during the severe acute respiratory syndrome coronavirus 2 (SARS-CoV-2) pandemic. *Respir Investig* Jan 2021;**59**(1):149–52 PubMed PMID: 33246913. Pubmed Central PMCID: PMC7667393. Epub 2020/11/29.
7. Anton A., Marcos M.A., Torner N., Isanta R., Camps M., Martinez A., et al. Virological surveillance of influenza and other respiratory viruses during six consecutive seasons from 2006 to 2012 in Catalonia, Spain. *Clin Microbiol Infect* Jun 2016;**22**(6):564e1–9 PubMed PMID: 26939538. Pubmed Central PMCID: PMC7172104. Epub 2016/03/05.
8. Chughtai A.A., Wang Q., Dung T.C., Macintyre C.R.. The presence of fever in adults with influenza and other viral respiratory infections. *Epidemiol Infect* Jan 2017;**145**(1):148–55 PubMed PMID: 27691995. Pubmed Central PMCID: PMC5197931. Epub 2016/10/04.
9. Ren L., Gonzalez A., Xu J., Xiao Y., Li Y., Zhou H., et al. Prevalence of human coronaviruses in adults with acute respiratory tract infections in Beijing. *China. J Med Virol* Feb 2011;**83**(2):291–7 PubMed PMID: 21181925. Pubmed Central PMCID: PMC7166607. Epub 2010/12/25.

Mei Dong, Ming Luo, Aihua Li, Hui Xie, Cheng Gong
Institute for immunization and prevention, Beijing Center for Disease Control and Prevention, Beijing Research Center for Preventive Medicine, No.16 Hepingli Middle Street, Dongcheng District, Beijing, PR China

Juan Du, Xinrui Wang
Department of Laboratorial Science and Technology, School of Public Health, Peking University, No.38 XueYuan Road, Haidian District, Beijing, PR China

Maozhong Li, Xue Wang, Yiting Wang
Institute for immunization and prevention, Beijing Center for Disease Control and Prevention, Beijing Research Center for Preventive Medicine, No.16 Hepingli Middle Street, Dongcheng District, Beijing, PR China

Haiyan Zhang
Institute for Infectious Diseases and Endemic Diseases Prevention and Control, Dongcheng Center for Disease Control and Prevention, No.5 Beibing Masi Hutong, Dongcheng District, Beijing, PR China

Xiaoxing Yang
Institute for Infectious Diseases and Endemic Diseases Prevention and Control, FengTai Center for Disease Control and Prevention, Kandan Science and Technology Industrial Park, Fengtai District, Beijing, PR China

Wei Cai
Institute for Infectious Diseases and Endemic Diseases Prevention and Control, Haidian Center for Disease Control and Prevention, No.5 Xibeiwang, 2nd Street, Haidian District (Health Building), Beijing, PR China

Hongjun Li
Institute for Infectious Diseases and Endemic Diseases Prevention and Control, Tongzhou Center for Diseases Prevention and Control, No.1 North Street, Luhe Middle School, Tongzhou District, Beijing, PR China

Wenzeng Zhang
Institute for Infectious Diseases and Endemic Diseases Prevention and Control, Shunyi District Centers for Disease Control and Prevention, No. 66 Shunkang Road, Shunyi District, Beijing, PR China

Lijun Ren
Institute for Infectious Diseases and Endemic Diseases Prevention and Control, Shijingshan Center for Disease Control and Prevention, No. 6 Stadium South Road, Shijingshan District, Beijing, PR China

Qing-Bin Lu*
Department of Laboratorial Science and Technology, School of Public Health, Peking University, No.38 XueYuan Road, Haidian District, Beijing, PR China

Fang Huang*
Institute for immunization and prevention, Beijing Center for Disease Control and Prevention, Beijing Research Center for Preventive Medicine, No.16 Hepingli Middle Street, Dongcheng District, PR China

*Corresponding authors at: Beijing Research Center for Preventive Medicine, Institute for immunization and prevention, Beijing Center for Disease Control and Prevention, No.16 Hepingli Middle Street, Dongcheng District, Beijing 100191, China.
E-mail addresses: qingbinlu@bjmu.edu.cn (Q.-B. Lu), hhffxdd@126.com (F. Huang)

Preserved C-reactive protein responses to blood stream infections following tocilizumab treatment for COVID-19

Dear editor,

In this Journal, Rossotti and colleagues provided early data on tocilizumab utility in COVID-19[1], later confirmed in randomised studies[2]. Tocilizumab-mediated inhibition of IL-6 signalling can decrease CRP concentrations[1], potentially confounding the diagnosis of bacterial co-infections in COVID-19 that occur more frequently following longer hospital stays and admissions to the intensive care unit (ICU)[3–5].

In inflammatory arthritides, serial tocilizumab dosing variably attenuates CRP responses following bacterial infections[6], but the effect following single-dose use in COVID-19 is not defined[2,7]. In a small COVID-19 cohort with blood stream infections (BSIs) that had received tocilizumab, CRP was reduced but remained detectable at the time of BSI diagnosis[8]. However, CRP kinetics related to BSI were not assessed, and thus the utility of CRP to guide antibiotic prescribing in this context remains unknown[5,9]. We addressed this question by testing the hypothesis that a single dose

Table 1
Baseline demographics and clinical characteristics for patients included in the study.

	No BSI & received tocilizumab(n = 90)	BSI & received tocilizumab(n = 17)	BSI & did not receive tocilizumab(n = 55)	p value*
Age, years, median (range)	63 (28–90)	61 (50–78)	63 (31–100)	p = 0.383
Gender, n (%)				
Male	56 (62)	9 (53)	38 (69)	p = 0.253
Female	34 (38)	8 (47)	17 (31)	
Ethnicity, n (%)				
White	33 (42)	4 (31)	27 (55)	p = 0.101
Black	7 (9)	3 (23)	7 (14)	
Asian	15 (19)	4 (31)	7 (14)	
Mixed	2 (3)	1 (8)	0 (0)	
Other	21 (27)	1 (8)	8 (16)	
Charlson co-morbidity score, n (%)				
0	57 (63)	4 (24)	27 (49)	p = 0.095
1	25 (28)	11 (65)	17 (31)	
2	6 (7)	1 (6)	7 (13)	
3+	2 (2)	1 (6)	4 (7)	
ICU admission, n (%)				
Yes	52 (58)	17 (100)	39 (72)	p = 0.015
No	38 (42)	0 (0)	15 (28)	
Corticosteroid use, n (%)				
Yes	79 (89)	15 (88)	35 (65)	p = 0.076
No	10 (11)	2 (12)	19 (35)	
BSI organism, n (%)				
Gram-negative bacilli	N/A	10 (40)	32 (62)	p = 0.507
Enterococcus sp.		2 (8)	12 (23)	
Staphylococcus aureus		4 (16)	7 (13)	
Other		1 (4)	1 (2)	

BSI = blood stream infection.

* relates to statistical comparison between COVID-19 patients who did or did not receive tocilizumab prior to the onset of BSI. Mann–Whitney test was used to compare age, Fisher's exact test was used to compare gender and microbiology results, and Chi-square test was used to compare ethnicity and Charlson co-morbidities.

of tocilizumab for COVID-19 retained CRP responses to bacterial infections, as modelled by BSIs.

We identified patients admitted to Royal Free Hospital (RFH) between 01/03/2020 and 01/02/2021, aged >18 years and diagnosed with COVID-19 by RT-PCR detection of SARS-CoV-2 from nasopharyngeal swabs. Tocilizumab use originated from routine clinical care delivery or randomised clinical trials after unblinding. COVID-19 associated BSIs were defined by isolation in blood cultures of any bacteria, excluding coagulase negative staphylococci, between 14 days prior to and 60 days after COVID-19 diagnosis. We excluded patients that developed BSIs prior to receiving tocilizumab. To assess dynamic CRP responses, we included only patients with blood parameter measurements performed at least 3 days prior to the onset of BSIs. Clinical, laboratory and drug data extraction, and statistical analyses were performed as previously described[5]. The study was approved by the Research and Innovation Group at RFH, which stated that as this was a retrospective review of routine clinical data, formal ethics approval was not required.

Within the COVID-19 patients that met our inclusion criteria, 107 had received tocilizumab, 17 of whom then developed a BSI during their hospital admission (Table 1). A separate cohort of 55 COVID-19 patients developed a BSI but had not received tocilizumab (Table 1). Tocilizumab use preceding BSIs was more commonly associated with ICU admission, but the BSI organisms were comparable between the groups (Table 1). In the first week after tocilizumab administration we observed a rapid fall in CRP (Fig. 1A), but not for total white cell, neutrophil or lymphocyte counts (Fig. 1A & fig S1). The CRP reduction following tocilizumab was short lived, with CRP concentrations rising within 21 days of tocilizumab receipt (Fig. 1A). To exclude confounding by bacterial co-infection, a sensitivity analysis on 90 patients that did not develop a BSI following tocilizumab also showed an early reduction followed by a rebound in CRP (fig S2A). A similar pattern was evident in patients that developed a BSI, although CRP concentrations showed less attenuation and greater heterogeneity within the 21-day period since tocilizumab administration (fig S2B).

To test the hypothesis that CRP would rise following a BSI independent of prior tocilizumab administration, we compared CRP responses in 17 patients that had received tocilizumab prior to a BSI with 55 patients who had not received tocilizumab. Strikingly, in both cohorts, BSIs resulted in clear CRP elevations (Figs. 1B & 1C). We calculated the change in CRP across the time of BSI onset to quantitatively compare this CRP rise. As blood samples were not collected daily in all patients, we derived paired sampling by calculating maximal CRP values 2 or 3 days prior to BSI-detecting blood culture collection and maximal CRP up to 2 days after BSI. This approach revealed an increase in CRP following BSI in 76.5% and 75.0% of patients that had or had not received tocilizumab respectively (Fig. 1D). Moreover, there was no difference in CRP increase between the groups (median CRP change +88 mg/L vs +76 mg/L respectively, $p = 0.67$ by Mann-Whitney test).

As patients developed BSIs at varying times following receipt of tocilizumab, we tested the hypothesis that BSI-induced CRP increment would be proportional to the time interval between tocilizumab administration and BSI onset. However, in the 17 patients that both received tocilizumab and subsequently developed a BSI, no relationship was observed between the length of the tocilizumab-BSI interval and the change in CRP ($r = 0.1069$, $p = 0.6811$ by Rank-spearman correlation) (Fig. 1E).

By inhibiting IL-6 signalling, tocilizumab may impact CRP-guided antibiotic prescribing decisions[5,9]. However, we demonstrate that prior administration of a single dose of tocilizumab does not attenuate CRP responses following a BSI, retaining the utility of this biomarker to diagnose bacterial co-infections associated with COVID-19. These findings have important implications for tocilizumab-treated COVID-19 patients: first, clinically-indicated antibiotic prescriptions are unlikely to be delayed, and second, low CRP levels alone are not an indication for continued prescription of unnecessary antibiotics, supporting stewardship efforts. Neverthe-
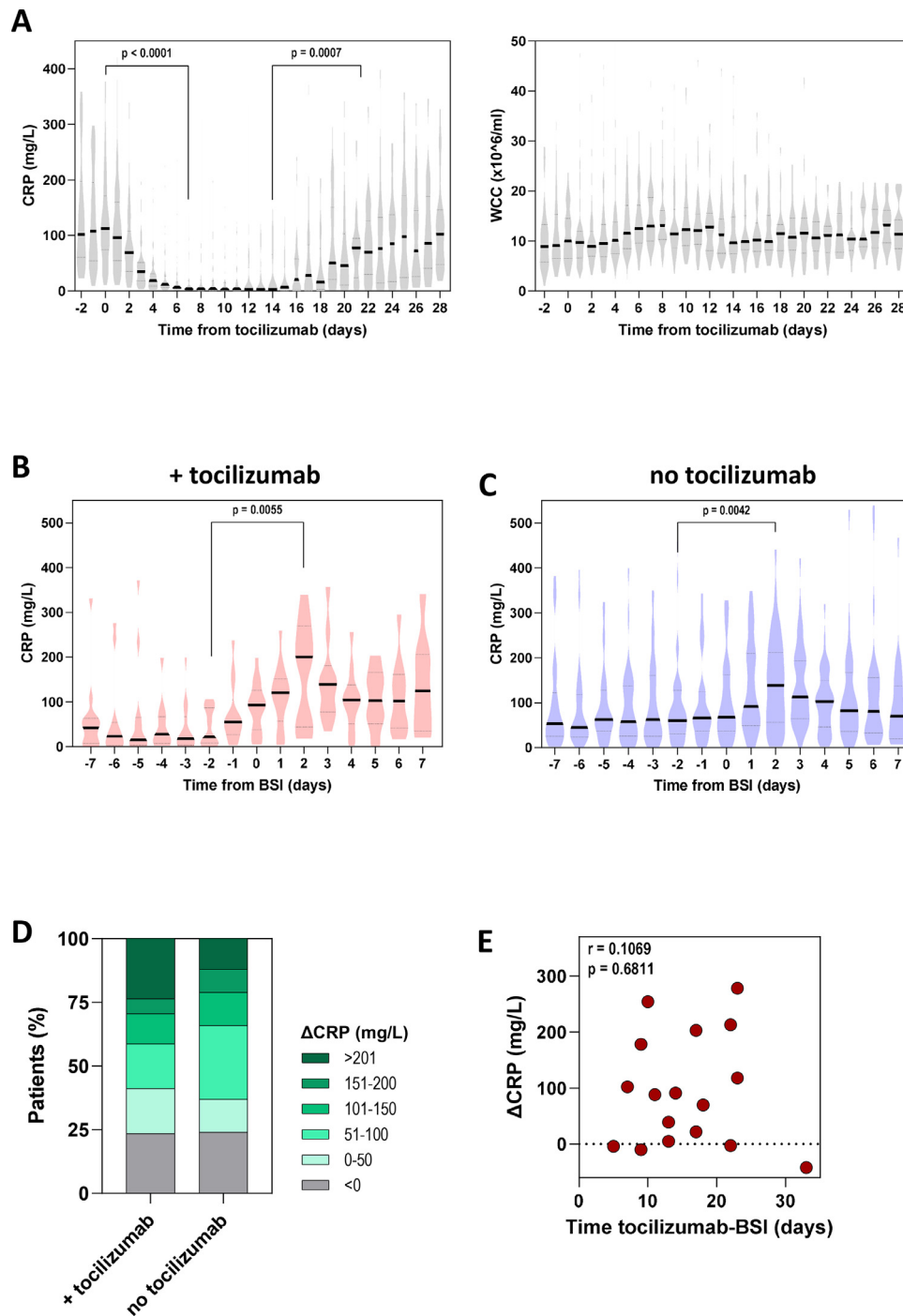
Fig. 1. Inflammatory marker responses following tocilizumab administration and onset of BSI in COVID-19. (A) CRP concentration (left panel) and white cell count (right panel) relative to time since tocilizumab administration. All COVID-19 patients receiving tocilizumab included in analysis, independent of a subsequent presence of BSI ($n = 107$). (B) CRP concentration over time in patients that received tocilizumab and subsequently developed a BSI ($n = 17$). (C) CRP concentration of time in COVID-19 patients that developed a BSI but with no prior tocilizumab exposure ($n = 55$). (D) Change (Δ) in CRP induced by onset of BSI in COVID-19 patients stratified by prior receipt of tocilizumab. (E) Relationship between ΔCRP induced by BSI and time between administration of tocilizumab and the onset of BSI. Violin plots represent frequency distribution of all samples, with bold and dashed lines representing median and quartile values. All p values were calculated by Mann-Whitney tests.

less, BSI onset did not initiate CRP elevations in all patients, irrespective of prior tocilizumab use, emphasising that CRP is only one contributor to diagnosing incipient bacterial infections.

Despite preserved CRP responses to BSI, tocilizumab transiently reduced baseline CRP levels, mostly recovering within 21 days. Furthermore, BSI-associated CRP increments were unrelated to time since tocilizumab, indicating that single tocilizumab dosing may not completely neutralise IL-6 responses[10], although a role for IL-

6-independent CRP stimuli cannot be excluded. Measuring IL-6 signalling activity in vivo may predict attenuation of CRP responses and also inform the need for further tocilizumab dosing in COVID-19[7].

Our study was limited by its single-centre and retrospective nature, constraining patient numbers and negating correction for potential confounders. Nevertheless, increased frequency of corticosteroid use in tocilizumab recipients could have further attenuated

CRP responses, counter to our observations. BSIs provided a standardised definition for bacterial infections, but limited extrapolation to non-BSI settings, an area of required future work to confirm the generalisability of our findings.

In conclusion, we show that tocilizumab use in severe COVID-19 preserves elevations in CRP concentration following the onset of a confirmed bacterial co-infection, as modelled by BSIs. Use of tocilizumab should not negate judicious, CRP-guided use of antibiotics in COVID-19.

Contributions

EQW, IB, SB and GP conceived the study. EQW, CB, AN, BOF, JP, ML, SY, SH, DM, MS and GP collected and analysed the data. EQW, SB and GP drafted the manuscript. All authors reviewed and approved the final version of the manuscript.

Declaration of Competing Interest

We declare that all authors have no conflicts of interest

Funding

No external funding supported this work.

Supplementary materials

Supplementary material associated with this article can be found, in the online version, at doi:10.1016/j.jinf.2021.08.017.

References

1. Rossotti R., Travi G., Ughi N., et al. Safety and efficacy of anti-il6-receptor tocilizumab use in severe and critical patients affected by coronavirus disease 2019: a comparative analysis. *J Infect* 2020;**81**(4):e11–17. doi:10.1016/j.jinf.2020.07.008.
2. RECOVERY Collaborative Group Tocilizumab in patients admitted to hospital with COVID-19 (RECOVERY): a randomised, controlled, open-label, platform trial. *Lancet* 2021;**397**(10285):1637–45. doi:10.1016/S0140-6736(21)00676-0.
3. Langford B.J., So M., Raybardhan S., et al. Bacterial co-infection and secondary infection in patients with COVID-19: a living rapid review and meta-analysis. *Clin Microbiol Infect* 2020;**26**(12):1622–9. doi:10.1016/j.cmi.2020.07.016.
4. Russell C.D., Fairfield C.J., Drake T.M., et al. Co-infections, secondary infections, and antimicrobial use in patients hospitalised with COVID-19 during the first pandemic wave from the ISARIC WHO CCP-UK study: a multicentre, prospective cohort study. *Lancet Microbe* June 2021. doi:10.1016/S2666-5247(21)00090-2.
5. Mason C.Y., Kanitkar T., Richardson C.J., et al. Exclusion of bacterial co-infection in COVID-19 using baseline inflammatory markers and their response to antibiotics. *J Antimicrob Chemother* January 2021. doi:10.1093/jac/dkaa563.
6. Lang V.R., Englbrecht M., Rech J., et al. Risk of infections in rheumatoid arthritis patients treated with tocilizumab. *Rheumatology (Oxford)* 2012;**51**(5):852–7. doi:10.1093/rheumatology/ker223.
7. Bell L.C.K., Meydan C., Kim J., et al. Transcriptional response modules characterize IL-1β and IL-6 activity in COVID-19. *iScience* 2021;**24**(1):101896. doi:10.1016/j.isci.2020.101896.
8. Giacobbe D.R., Battaglini D., Ball L., et al. Bloodstream infections in critically ill patients with COVID-19. *Eur J Clin Invest* 2020;**50**(10):e13319. doi:10.1111/eci.13319.
9. Seaton R.A., Gibbons C.L., Cooper L., et al. Survey of antibiotic and antifungal prescribing in patients with suspected and confirmed COVID-19 in Scottish hospitals. *J Infect* 2020;**81**(6):952–60. doi:10.1016/j.jinf.2020.09.024.
10. Spencer S., Köstel Bal S., Egner W., et al. Loss of the interleukin-6 receptor causes immunodeficiency, atopy, and abnormal inflammatory responses. *J Exp Med* 2019;**216**(9):1986–98. doi:10.1084/jem.20190344.

Emmanuel Q. Wey
Department of Infection, Royal Free London NHS Trust, London, United Kingdom
Centre for Clinical Microbiology, Division of Infection & Immunity, UCL, London, United Kingdom

Clare Bristow
Department of Infection, Royal Free London NHS Trust, London, United Kingdom

Aarti Nandani, Bryan O'Farrell, Jay Pang, Marisa Lanzman
Department of Pharmacy, Royal Free London NHS Trust, London, United Kingdom

Shuang Yang
Clinical Practice Group, Analysis Division, Transplant and Specialist Services & Women and Children, Royal Free London NHS Trust, London, United Kingdom

Soo Ho, Damien Mack
Department of Infection, Royal Free London NHS Trust, London, United Kingdom

Michael Spiro
Division of Surgery and Interventional Science, University College London, United Kingdom

Indran Balakrishnan, Sanjay Bhagani
Department of Infection, Royal Free London NHS Trust, London, United Kingdom

Gabriele Pollara[*]
Department of Infection, Royal Free London NHS Trust, London, United Kingdom
Division of Infection & Immunity, University College London, United Kingdom

[*]Corresponding author at: Division of Infection & Immunity, University College London, United Kingdom
E-mail address: g.pollara@ucl.ac.uk (G. Pollara)

Are COVID-19 susceptibility genes related to lung cancer?

Dear editor,

We read with great interest the recently published letter in *Journal of Infection* by Afshar et al., who suggested that the proportion of severe cases and mortality among cancer patients infected with COVID-19 were higher than those of COVID-19 patients without cancer, due to abnormal autoimmune function.[1] Meanwhile, Liang et al. collected and analyzed 2007 cases from 575 hospitals in China who were diagnosed with COVID-19 and were admitted to hospital for treatment, and found that 1% of COVID-19 patients had a history of cancer, which was much higher than the incidence of cancer in the normal population (0.29%).[2] However, the COVID-19 susceptibility of cancer patients remains a subject of considerable controversy. Observational studies with different samples have even come to opposite conclusions. Gallo et al. suggested that the impaired immune response of cancer patients might be a protective factor for the cytokine storm caused by COVID-19.[3] Therefore, it is necessary to discuss whether susceptibility genes for COVID-19 play a critical role in lung cancers.

In this study, we comprehensively analyzed the genetic alteration, mRNA expression, protein expression, prognosis, immune infiltration and lung cancer correlation of COVID-19 susceptibility genes (*SLC6A20, LZTFL1, CCR9, FYCO1, CXCR6, XCR1, ABO, RPL24,*

Table 1
Differentially expressed genes in the lung cancer patient cohort of ONCOMINE database.

Gene	Fold Change	P	Cancer type	Study	Sample
LZTFL1	1.658	0.009	Small Cell Lung Carcinoma	Garber Lung	73
TMEM65	1.738	0.001	Squamous Cell Lung Carcinoma	Garber Lung	73
OAS1	3.416	3.00E-4	Lung Adenocarcinoma	Bhattacharjee Lung	203
DPP9	2.123	0.004	Large Cell Lung Carcinoma	Garber Lung	73
RAVER1	1.795	7.92E-17	Lung Adenocarcinoma	Selamat Lung	116
IFNAR2	2.027	1.64E-14	Lung Adenocarcinoma	Selamat Lung	116

Only genes that were considered to be differentially expressed were shown. The statistically significant differential expression is defined to be $P < 0.05$ and Fold Change > 1.5.
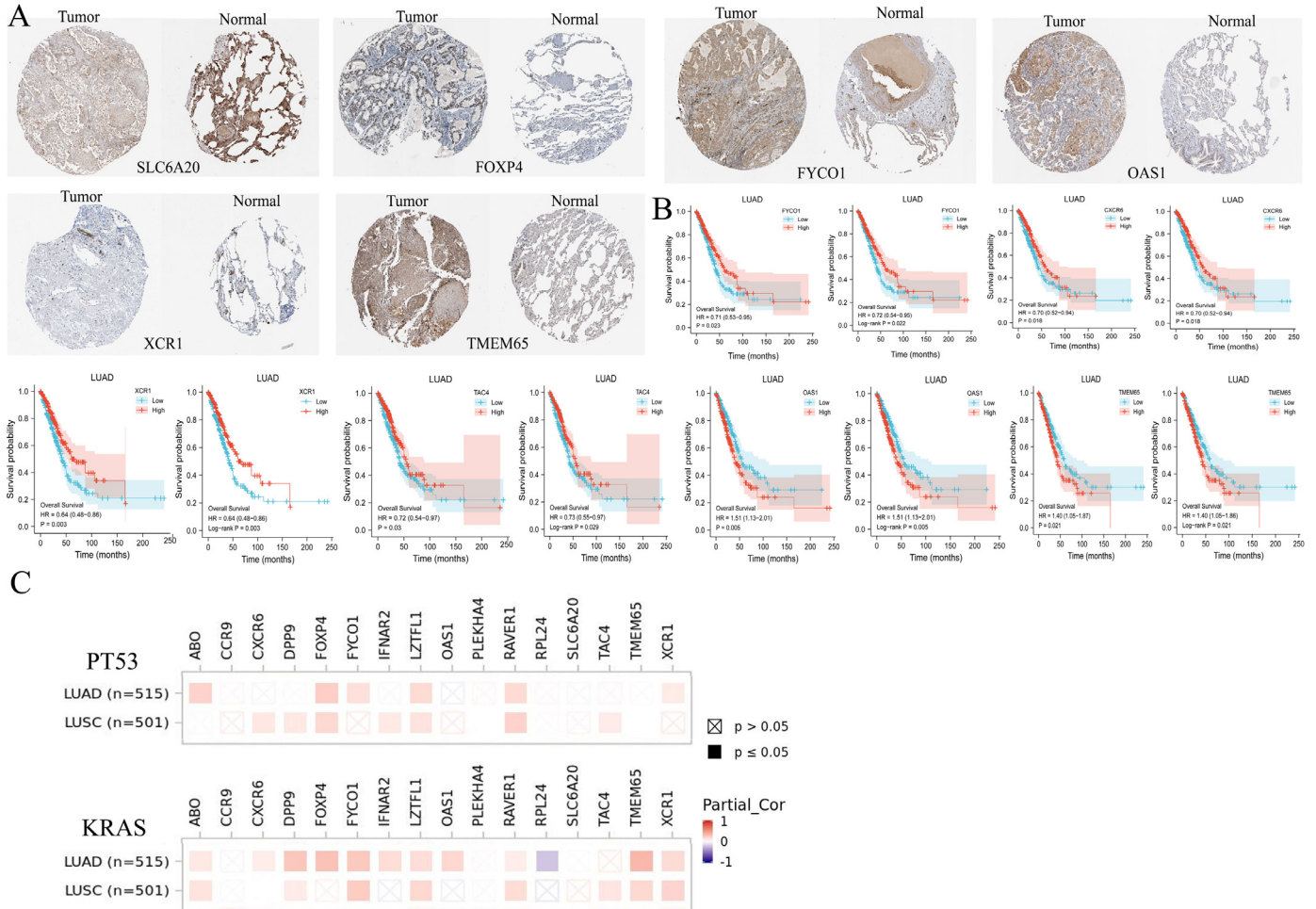

Fig. 1. The protein expression, prognosis, and lung cancer correlation of COVID-19 susceptibility genes. (A) Representative immunohistochemical staining in lung tumor and normal tissues. (B) Survival curves compared the overall survival of COVID-19 susceptibility genes expression using the cox regression model and log rank test. (C) Correlation of COVID-19 susceptibility genes expression with lung cancer markers.

FOXP4, TMEM65, OAS1, KANSL1, TAC4, DPP9, RAVER1, PLEKHA4 and *IFNAR2*) in lung adenocarcinoma (LUAD) and lung squamous cell carcinoma (LUSC).[4] Among the 17 susceptibility genes, the genetic alteration of *RPL24* was as high as 6.37% in LUSC and the genetic alteration of *TMEM65* was as high as 5.48% in LUAD, suggesting that genetic alteration in these genes greatly affected the occurrence of lung cancer. Most of COVID-19 susceptibility genes were differential expression in samples of TCGA lung cancer datasets, and the differential expression of *LZTFL1, TMEM65, OAS1, DPP9, RAVER1* and *IFNAR2* were replicated in three cohort studies (**Table 1**). Using immunohistochemical staining to validate the protein expression of lung cancer tissues and normal lung tissues in the Human Protein Atlas, we observed that six genes, including

SLC6A20, FYCO1, FOXP4, TMEM65, XCR1 and *OAS1*, had significantly different protein expression levels (**Fig. 1A**).

Subsequently, we used the cox regression model and log rank test to calculate the impact of COVID-19 susceptibility gene expression in overall survival (OS). Whether under the cox model or log rank test, high expression of *FYCO1, CXCR6, XCR1* and *TAC4* were protective factors for LUAD, and *TMEM65* and *OAS1* were risk factors for LUAD (**Fig. 1B**). Finally, we were pleasantly surprised to find that COVID-19 susceptibility genes were strongly related to almost all of the six main immune cells (B cell, CD8+ T cell, CD4+ T cell, macrophage, neutrophil and dendritic cell) in lung cancer, further confirming the close interaction of COVID-19 with immune responses in tumors. We also explored the association between COVID-19 susceptibility genes and known markers of lung cancer

(*P53→TP53* and *KRAS*) in lung cancer. *ABO, DPP9, FOXP4, FYCO1, LZTFL1, RAVER1, TAC4* and *XCR1* were strongly correlated with both lung cancer markers (**Fig. 1**C).

In conclusion, we verified the results of COVID-19 Host Genetics Initiative that individuals with mutations in these two genes related to lung cancer, *DPP9* and *FOXP4*, increased the risk of severe COVID-19[4]. Furthermore, we suggested *XCR1, TMEM65* and *OAS1* as independent prognostic markers for lung cancer, and supported the potential partial genetic overlap between COVID-19 and lung cancer. We provided new insights and research directions for the diagnosis, treatment and management of lung cancer patients during the COVID-19 pandemic.

Declaration of Competing Interest

All the authors declare that there are no conflicts of interest.

Acknowledgement

References

1. Afshar Z.M., Dayani M., Naderi M., Ghanbarveisi F., Shiri S., Rajati F.. Fatality rate of COVID-19 in patients with malignancies: a sytematic review and meta–analysis. *J Infect* 2020;**81**(2):e114–e1e6 AugPubMed PMID: 32474042. Pubmed Central PMCID: PMC7255731 conflicts of interest. Epub 2020/06/01.
2. Liang W., Guan W., Chen R., Wang W., Li J., Xu K., et al. Cancer patients in SARS-CoV-2 infection: a nationwide analysis in China. *Lancet Oncol* 2020;**21**(3):335–7 MarPubMed PMID: 32066541. Pubmed Central PMCID: PMC7159000. Epub 2020/02/19.
3. Gallo O., Locatello L.G., Orlando P., Martelli F., Piccica M., Lagi F., et al. Cancer population may be paradoxically protected from severe manifestations of COVID-19. *J Infect* 2020;**81**(2):e156–e1e8 AugPubMed PMID: 32534002. Pubmed Central PMCID: PMC7286269. Epub 2020/06/14.
4. Initiative C.H.G.. Mapping the human genetic architecture of COVID-19. *Nature* 2021 PubMed PMID: 34237774. Epub 2021/07/09. https://www.nature.com/articles/s41586-021-03767-x.

Shizheng Qiu
Yang Hu*
School of Life Science and Technology, Harbin Institute of Technology, No. 2 Yikuang Street, Nangang District, Harbin 150001, China
Corresponding author.
E-mail address: huyang@hit.edu.cn (Y. Hu)

Long-lasting immune response to a mild course of PCR-confirmed SARS-CoV-2 infection: A cohort study

Dear editor,

We read with great interest the paper by Wells et al..[1] Wells et al. investigated seroprevalence of SARS-CoV-2 antibodies in a cohort of 431 non-hospitalized UK twins (mean age = 48.38, SD = 28; 85.1% female), who systematically reported the presence or absence of COVID-19 symptoms on many occasions through time via an ad-hoc study app. Their results indicated that 51 of the 431 individuals (11.8%) were seropositive with IgG response to both N and S proteins 4-fold above the background of the assay. Within the group of seropositive individuals with complete symptom data (*n* = 48), there were 35 participants (72.9%) with core symptoms (defined as anosmia, cough and fever) and 13 (27.1%) without core symptoms. Among these 13, 9 (18.7%) participants were fully asymptomatic. This finding is particularly relevant, as it shows that also participants with an asymptomatic course of the disease developed antibodies against SARS-CoV-2. While the longitudinal assessment of symptoms with the app allowed to track the clinical course of the disease, a major limitation of the study by Wells et al.[1] is that SARS-CoV-2 infection was not confirmed by real-time polymerase chain reaction (RT-PCR) at symptom onset. Therefore, the time interval between infection and sample collection was unknown. This is an important source of variability that likely affected the estimated percentage of seropositive individuals. Moreover, the cohort comprised related individuals (twins), whose immune response to exposure to SARS-CoV-2 was probably correlated to some extent.[2] It follows that observations were not independent and this probably affected results. Nevertheless, the idea of studying the immune response against SARS-CoV-2 in individuals who underwent a mild course of COVID-19 is of pivotal importance, because mild cases represent the most typical manifestation of this disease and many infections are even asymptomatic.[3,4] Previous studies described the longitudinal stability of immunity against SARS-CoV-2 mostly in hospitalized COVID-19 patients with mixed clinical profiles (mild, moderate or severe symptoms), using different laboratory methods for the analysis of antibodies (see for example[5–9]). Therefore, knowledge about the longitudinal stability of the immune response in mild and asymptomatic SARS-CoV-2 infections is limited.

We present recent findings from a cohort of COVID-19 convalescent individuals that partly replicate and extend the evidence by Wells et al.[1] We collected blood plasma samples to determine pan-IG antibody titre from a cohort of 326 non-hospitalized volunteers (median age = 42 years, IQR = 31–52; 61.7% females) tested positive for SARS-CoV-2 by RT-PCR between February 2020 and January 2021. Samples of serum, lithium heparin plasma, sodium citrate plasma, EDTA plasma and EDTA buffy coat were collected at the baseline visit after remission of SARS-CoV-2 infection (median = 66 days, IQR = 42.0–111.8 between infection and baseline visit) and 1, 2, 5 and 12 months after the baseline visit. Clinical symptoms of COVID-19, demographic characteristics, lifestyle, and comorbidities were collected by study physicians via an electronic questionnaire at the baseline visit. Antibody levels were determined with the Elecsys® Anti-SARS-CoV-2 (pan-Ig qualitative test against the viral nucleocapsid protein, positive if ≥ 1 COI) and the Elecsys®Anti-SARS-CoV-2 S assays (pan-Ig quantitative test against the receptor-binding domain of the viral spike protein S1-ab, positive if ≥ 0.8 U/ml) (Roche Diagnostics, Rotkreuz, Switzerland). Data and sample collection for late timepoints is still ongoing. Samples collected after the date of first vaccination were censored.

Overall, 300 (92.0%) participants experienced COVID-19 core symptoms (at least one among fever, cough, dyspnea, ageusia and anosmia during the course of the disease), 26 (8.0%) did not; 88 participants (27.0%) presented with comorbidities and they were equally distributed among individuals with/without core symptoms. A clinically relevant finding is the high proportion of individuals with long-lasting symptoms: After a median time of 38 days post infection (IQR = 14–84 days), 218 participants (66.9%) still had symptoms. The most common were fatigue (*N* = 134, 41.1%), dysgeusia (*N* = 77, 23.6%), headache (*N* = 76, 23.3%), anosmia (*N* = 65,

Table 1.

Results of the quantitative antibody assay (U/ml) in the whole cohort and in each subgroup.

	Baseline (Visit 1)		Visit 2		Visit 3		Visit 4	
	N	Median (Q1, Q3)	N	Median (Q1, Q3)	N	Median (Q1, Q3)	N	Median (Q1, Q3)
Whole cohort	320*	48.7 (14.9, 161.0)	241	68.8 (27.7, 189.0)	146	94.7 (37.6, 311.5)	90	131.5 (51.3, 421.5)
Participants with early baseline visit	84	11.4 (3.0, 35.8)	74	36.5 (12.8, 89.5)	35	37.3 (16.8, 95.8)	2	42.2 (41.0, 43.5)
Participants with late baseline visit	236	72.2 (27.5, 213.0)	167	89.2 (37.8, 300.0)	111	115.0 (49.9, 381.5)	88	132.5 (59.9, 437.0)
Participants with core symptoms	296	50.0 (16.5, 173.8)	223	70.5 (29.2, 209.5)	137	94.9 (38.4, 314.0)	86	144.0 (50.0, 467.0)
Participants without core symptoms	24	27.6 (2.1, 83.0)	18	45.8 (7.2, 83.9)	9	56.1 (28.4, 95.7)	4	76.5 (71.3, 90.5)
Participants without comorbidities	235	39.4 (12.2, 111.5)	176	50.4 (22.1, 146.8)	107	77.1 (32.4, 250.0)	61	117.0 (42.7, 415.0)
Participants with comorbidities	85	94.1 (42.6, 232.0)	65	122.0 (55.8, 319.0)	39	177.0 (80.3, 434.5)	29	221.0 (79.9, 579.0)

Note. Visits 2, 3, 4 occurred 1, 2, 5 months after the baseline (visit 1), respectively. * Five observations were censored due to vaccination already at baseline (visit 1). The value of the quantitative antibody assay of the first visit was missing for one participant.
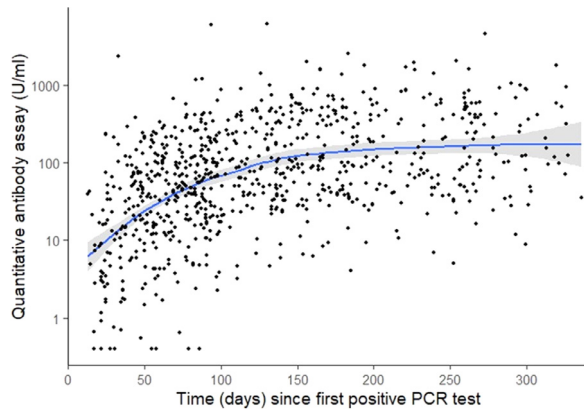

Fig. 1. Kinetics of the antibody response as a function of time since the first positive PCR test. Antibody levels are shown on a log10-scale on the y-axis. The blue line (with a gray band for the 95% confidence interval) is the output of Local Polynomial Regression Fitting (LOESS). Please note that, to improve data visualization, one observation at day 360 was excluded from the plot.

19.9%), nasal congestion ($N = 56$, 17.2%) and dyspnea ($N = 54$, 16.6%).

Results of antibody tests revealed very high positivity rates (qualitative assay at baseline visit positive in 303 of 321[1] individuals, 94.4%; quantitative antibody assay at baseline visit positive in 310 of 320[2] individuals, 96.9%) and these increased through time, reaching 96.7% and 100% positivity rates by visit 4 for the qualitative and the quantitative assays, respectively.

To account for variability in the time lag between the first PCR test and the baseline visit (visit 1), participants were subdivided into 2 groups: Individuals with baseline visit within 42 days since the first PCR test (early baseline visit group) and individuals with baseline visit occurring more than 42 days since the first PCR test (late baseline visit group). Table 1 shows median (IQR) of the quantitative antibody assay in the whole cohort (see also Fig. 1) and in the different subgroups. We modeled the longitudinal variation of quantitative antibody titres through time with linear mixed effects models, adding a random intercept and a random slope to account for the random variation of individual time trajectories. Results revealed a significant positive association between log-transformed antibody quantitative titre and time since the first PCR test (estimate = 1.07, $p < 0.001$). The effect of the baseline visit group was also significant: The late group generally had higher antibody levels than the early group (estimate = 1.38, $p < 0.001$). The presence of core symptoms (estimate = 0.52, $p < 0.001$) and of comorbidities (estimate = 0.30, $p < 0.001$) was related to higher antibody levels. The interaction between time and the early/late baseline visit group was significant (estimate = −0.61, $p < 0.001$), indicating that the increase in the antibody levels was steeper in the early vs. late baseline group.

Taken together, our results indicate a strong and persistent immune response against SARS-CoV-2 infection in individuals who recovered from a mild course of COVID-19 for up to 8 months post infection. Importantly, our findings are in line with a recent study[10] that used the very same quantitative anti-RBD antibody assay as we did and reported a robust and persistent antibody response after six months post infection. The titre at the baseline visit and its change through time was modulated by the time lag between infection and sampling. In line with Wells et al., we found that individuals without core symptoms developed immunity against COVID-19, although to a lower degree than individuals showing core symptoms, and it persisted through time.

In the framework of this ongoing pandemic, our study highlights the importance of high quality research data that arise from patient and sample collections of biorepositories.

Declaration of Competing Interest

The authors declare no conflict of interest.

Ethics approval

The study was performed in accordance with the latest version of the Declaration of Helsinki and was approved by the local ethics committee of the Medical University of Graz (ethics vote: 32–423 ex 19/20) All participants signed a Biobank-informed consent and a study-specific informed consent.

Funding

Acknowledgments

References

1. Wells P.M., Doores K.J., Couvreur S., Nunez R.M., Seow J., Graham C., et al. Estimates of the rate of infection and asymptomatic COVID-19 disease in a population sample from SE England. *J Infect* 2020;**81**(6):931–6 Dec.
2. Brodin P., Jojic V., Gao T., Bhattacharya S., Angel C.J., Furman D., et al. Variation in the human immune system is largely driven by non-heritable influences. *Cell* 2015;**160**(1–2):37–47 Jan 15.

---

[1] Five observations were censored due to vaccination already at baseline (visit 1).

[2] The value of the quantitative antibody assay of the first visit was missing for one participant.

3. Tian S., Hu N., Lou J., Chen K., Kang X., Xiang Z., et al. Characteristics of COVID-19 infection in Beijing. *J Infect* 2020;**80**(4):401–6 Apr.
4. Wu Z., McGoogan J.M.. Characteristics of and important lessons from the coronavirus disease 2019 (COVID-19) outbreak in China: summary of a report of 72314 cases from the chinese center for disease control and prevention. *JAMA* 2020;**323**(13):1239–42 Apr 7.
5. Seow J., Graham C., Merrick B., Acors S., Pickering S., Steel K.J.A., et al. Longitudinal observation and decline of neutralizing antibody responses in the three months following SARS-CoV-2 infection in humans. *Nat Microbiol* 2020;**5**(12):1598–607 Dec.
6. Secchi M., Bazzigaluppi E., Brigatti C., Marzinotto I., Tresoldi C., Rovere–Querini P., et al. COVID-19 survival associates with the immunoglobulin response to the SARS-CoV-2 spike receptor binding domain. *J Clin Invest* 2020;**130**(12):6366–78 Dec 1.
7. Long Q.X., Liu B.Z., Deng H.J., Wu G.C., Deng K., Chen Y.K., et al. Antibody responses to SARS-CoV-2 in patients with COVID-19. *Nat Med* 2020;**26**(6):845–8 Jun.
8. Dehgani-Mobaraki P., Kamber Zaidi A., Porreca A., Floridi A., Floridi E., Monti M., et al. Antibody persistency and trend post-SARS-CoV-2 infection at eight months. *Ann Ig* 2021 Jun 11. doi:10.7416/ai.2021.2455.
9. Dispinseri S., Secchi M., Pirillo M.F., Tolazzi M., Borghi M., Brigatti C., et al. Neutralizing antibody responses to SARS-CoV-2 in symptomatic COVID-19 is persistent and critical for survival. *Nat Commun* 2021;**12**(1):2670 May 11021-22958-8.
10. L'Huillier A.G., Meyer B., Andrey D.O., Arm-Vernez I., Baggio S., Didierlaurent A., et al. Antibody persistence in the first 6 months following SARS-CoV-2 infection among hospital workers: a prospective longitudinal study. *Clin Microbiol Infect* 2021;**27**:784.e1–784.e8 Jan 20.

Sabrina Kral*[1]
Biobank Graz, Medical University of Graz, Graz, Austria

Chiara Banfi[1]
Institute for Medical Informatics, Statistics and Documentation, Medical University Graz, Graz, Austria

Tobias Niedrist
Clinical Institute of Medical and Chemical Laboratory Diagnostics, Medical University of Graz, Graz, Austria

Nazanin Sareban
Department of Blood Group Serology and Transfusion Medicine, Medical University of Graz, Graz, Austria

Christian Guelly
Biobank Graz, Medical University of Graz, Graz, Austria
Center for Medical Research, Medical University of Graz, Graz, Austria

Lisa Kriegl
Division of Infectious Diseases, Department of Internal Medicine, Medical University of Graz, Graz, Austria

Stefanie Schiffmann
Department of Blood Group Serology and Transfusion Medicine, Medical University of Graz, Graz, Austria

Christoph Zurl
Division of Infectious Diseases, Department of Internal Medicine, Medical University of Graz, Graz, Austria
Division of General Paediatrics, Department of Paediatrics and Adolescent Medicine, Medical University of Graz, Graz, Austria
BioTechMed-Graz, Graz, Austria

Markus Herrmann
Clinical Institute of Medical and Chemical Laboratory Diagnostics, Medical University of Graz, Graz, Austria

Ivo Steinmetz
Diagnostic and Research Institute of Hygiene, Microbiology and Environmental Medicine, Medical University of Graz, Graz, Austria

Peter Schlenke
Department of Blood Group Serology and Transfusion Medicine, Medical University of Graz, Graz, Austria

Andrea Berghold

Institute for Medical Informatics, Statistics and Documentation, Medical University Graz, Graz, Austria

Robert Krause
Division of Infectious Diseases, Department of Internal Medicine, Medical University of Graz, Graz, Austria
BioTechMed-Graz, Graz, Austria

*Corresponding author.
E-mail address:* sabrina.kral@medunigraz.at (S. Kral)

[1] These authors contributed equally to this work.

Clinical, radiographic features and long-term outcomes of paradoxical cryptococcosis-associated immune reconstitution inflammatory syndrome secondary to the ventriculoperitoneal shunt

Dear Editor

Paradoxical immune reactions in cryptococcal meningitis (CM), also termed as cryptococcal-immune reconstitution inflammatory syndrome (C-IRIS), occurs in 13%–30% of immunodeficiency individuals with CM receiving antifungal therapy and antiretroviral therapy(ART).[1,2] However, in recent years, isolated cases and small case series of IRIS have also been reported in immunocompetent CM hosts with varying frequencies.[3,4] IRIS manifestations include deterioration of clinical manifestations and neuroimaging abnormalities, as well as changes in cerebrospinal fluid after clinical and/or microbial responses to anti-cryptococcal therapy. Case reports and small case series reported the use of ventriculoperitoneal shunt (VPS) to treat uncontrollable intracranial hypertension in patients with cryptococcal meningitis with or without hydrocephalus.[5] In this study, we observed the clinical, neuroimaging and cerebrospinal fluid changes in non-HIV CM patients after VPS. Our findings reveal the frequency of paradoxical immune reactions after VPS and its impact on the long-term outcome.

This prospective and observational study was conducted in the Department of Neurology, the Third Affiliated Hospital of Sun Yat-sen University from January 2012 to March 2017. We included 25 patients who newly diagnosed with HIV-negative cryptococcal neoformans meningitis and received VP shunt due to uncontrollable intracranial hypertension or further deterioration of neurological conditions. Patients will be excluded if they have a history of autoimmmune disease or use immunosuppressive medications. All patients received continuous antifungal therapy (amphotericin B, diflucan and 5-fluorocytosine) before and after shunting. Patients were followed up regularly for 24 months after VPS. Clinical evaluation, CSF analysis and neuroimaging examination were completed at a regular time or during clinical deterioration. The modified Rankin scale (6-point scoring system) is used to assess disability.

In our study, 22 cases (88%) of CM patients experienced IRIS after VPS. Compared with paradoxical changes in neuroimaging and clinical manifestation, paradoxical CSF reactions are more common (76%, 68%, 88%, respectively). The most common clinical paradoxical reaction after VPS is headache (44%). Others include fever, fatigue, delirium, confusion, seizures, etc. Paradoxical neuroimag-
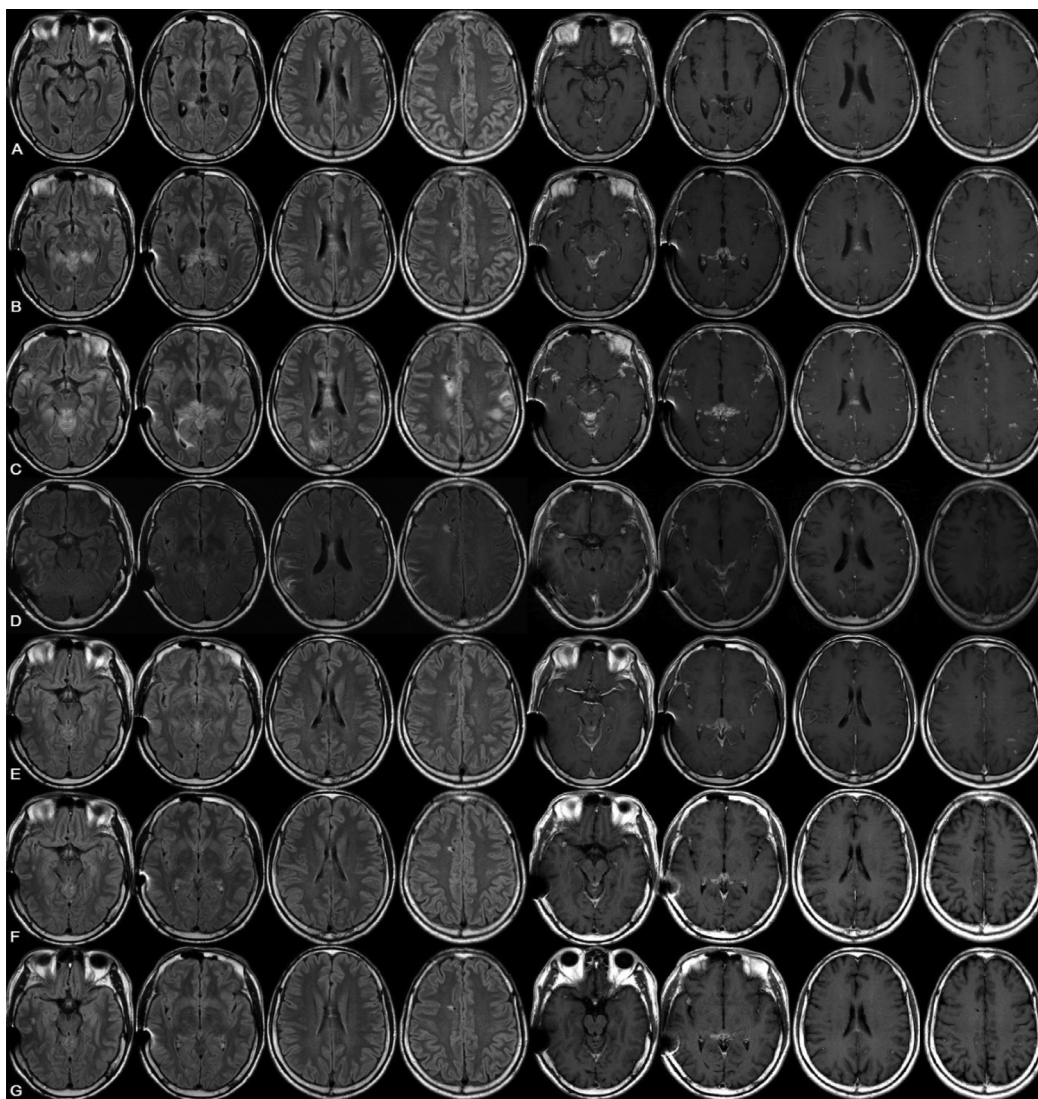
Fig. 1. The radiologic spectrum of imaging paradoxical manifestations. Serial axial cranial T2 FLAIR and post-contrast T1 weighted images in representative case (patient 11). A, MR images before VPS showed leptomeningeal enhancement in the right parietal region. B, MR images 1.5 month after VPS showed more leptomeningeal enhancement and new lesions in thalamus and corpora quadrigemina. C, MR images 2.5 month after VPS showed the deterioration of the previous manifestation and development of additional cryptococcoma and new lesions in occipital lobe. D, MR images 5 month after VPS showed the improvement after corticosteroid treatment. Follow-up imaging at 13 month after VPS (E), 25 month after VPS (F) and 31 month after VPS (G).

ing changes include worsening leptomeningeal enhancement (76%), new parenchymal brain lesions (60%), white matter lesions (56%) and new or existing enlarged cryptococcoma (20%), etc. The time for neuroimaging deterioration after VPS is 30 to 60 days, and the time for improvement of paradoxical neuroimaging lesions is 60 days to 12 months (median 4 months). Representative paradoxical neuroimaging changes in patient 11 were showed in Fig. 1. Paradoxical deterioration of cerebrospinal fluid after VPS include increased protein levels (88%), decreased glucose levels (40%), leukocytosis (56%) and/or shift towards polymorphonuclear pleocytosis (40%) (Table 1). These changes usually peak within 24 weeks after VPS. In patient 11, paradoxical CSF changes lasted for more than 22 months after the cryptococcal culture was negative, but his clinical manifestations improved 2 months after VPS.

In the IRIS group, 14 patients (63.6%) were completely improved, while 7 patients (31.8%) had a moderate outcome and 1 patient (4.5%) had a poor outcome. 5 patients with severe IRIS were misdiagnosed as alternative central nervous system infections, such as bacterial or tuberculosis infection after VPS. Nine patients with severe IRIS were injected with prednisone (0.75–

1.5 mg/kg/day) or dexamethasone (10–20 mg/day) for 7–10 days, and then gradually reduced oral low-dose prednisone for 7 days. Seven patients improved only after receiving corticosteroids therapy. Two patients received prolonged prednisone treatment for persistent headache, significant elevation of CSF protein and diffuse brain lesions, which were 22 months for patient 11 and 4 months for patient 23, respectively.

Discussion

The reports have shown that the incidence of C-IRIS related to ART is 13%−30%.[1,6] However, in our study, 88% of non-HIV CM patients had paradoxical IRIS after VP shunt. The most important finding of our research is that VPS-related IRIS are very common. Among paradoxical IRIS, CSF paradoxical reactions are more common than paradoxical neuroimaging changes and paradoxical clinical manifestations. Most studies have shown that ART-related CM-IRIS in HIV patients occurs 1–2 months after the initiation of ART.[1,7] In our study, clinical paradoxical changes usually occur within a few days after VP shunt. Paradoxical neuroimaging deteri-

Table 1
Summary of the changes in the 22 cryptococcal meningitis patients with IRIS after the VP shunt.

	IRIS group ($n = 22$)
Overall paradoxical reaction, n (%)	22 (88%)
Clinical paradoxical reaction, n (%)	17 (68%)
Headache	11 (44%)
Fever	10 (40%)
Hallucination	5 (20%)
Fatigue	5 (20%)
Worsening consciousness level	3 (12%)
Visual impairment	3 (12%)
Seizure	2 (8%)
CSF paradoxical reaction, n (%)	22 (88%)
High CSF leukocyte count	14 (56%)
High CSF protein	22 (88%)
Low CSF glucose	10 (40%)
Shift towards polymorphonuclear pleocytosis	10 (40%)
Neuroimaging paradoxical reaction in brain, n (%)	19 (76%)
Worsening of leptomeningeal enhancement	19 (76%)
New parenchymal lesion	15 (60%)
New white matter lesion	14 (56%)
New cerebeller lesions	6 (24%)
New or existing enlarged cryptococcoma	5 (20%)
New brain stem lesion	5 (20%)
Spinal involvement	5 (20%)
Worsening of hydrocephalus	5 (20%)
Worsening of vasculitis	2 (8%)
Steriod used in the IRIS group, n (%)	9 (36%)

IRIS=immune reconstitution inflammatory syndrome; VP=ventriculoperitoneal; CSF=cerebrospinal fluid.

orations occur 30 to 60 days after VP shunt, and improve from 60 days to 12 months (median 4 months) after VP shunt. Paradoxical CSF changes usually peak 2–4 weeks after VPS, and may persist for more than 4 months after CSF cryptococcal culture is negative. In patient 11, the paradoxical neuroimaging and CSF abnormality lasted more than 22 months after the cryptococcal culture was negative, although he was clinically responsive to antifungal therapy and corticosteroid therapy. These three paradoxical reactions will not occur or recover simultaneously. Paradoxical neuroimaging and CSF changes last longer than paradoxical clinical reactions. This inconsistency makes IRIS after VP shunt may be misdiagnosed as treatment failure or alternative CNS infection.

The pathogenesis of CM-IRIS in HIV and non-HIV patients is still poorly understood. The pathogenesis of ART-related CM-IRIS in HIV patients is related to the immune restoration after ART treatment. Antifungal-induced CM-IRIS in immunocompetent hosts has been proved to have a similar immune response to ART-related IRIS. IRIS occurs when antifungal therapy reverses the immunosuppressive state mediated by Th2 phenotypic response.[8] In our study, timing, changes in CSF and neuroimaging, and good response to steroid therapy indicate that the immune response involves VPS-related IRIS. The main risk factor may be related to the high cryptococcal load before VPS and the rapid decline after VPS. Compared with the non-IRIS group, the IRIS group had much higher quantitative CSF cryptococcal counts before shunt (medium 15,141 vs. 2603 numbers/mL, $p = 0.016$) and shorter CSF culture-negative time after shunt (medium 39.9 vs. 150 days, $p = 0.000$). The results show that the pathogenesis of VPS-related IRIS is similar to the immune restoration syndrome in ART-related IRIS. The immune pathogenesis and prediction of CM-IRIS after VPS are still unclear, and it is worthy of further study. There are no controlled clinical trials for the management of CM-IRIS. Recent reports indicate that there is a good response to corticosteroids in ART-related CM-IRIS or antifungal-induced CM-IRIS.[9,10] Our results also show that corticosteroid therapy is a good choice for VPS-related IRIS and will not cause CM recurrence. The dose and duration of corticosteroids

are still inconclusive, and they are usually individualized based on clinical response.

VP shunt placement is an effective method to continuously relieve uncontrolled ICP, so it is essential to improve the survival rate and neurological function of CM patients. IRIS related to VPS is very common. Recognizing that these reactions are the result of an immune response, not a treatment failure or alternative diagnosis, is important to avoid inappropriate changes in treatment.

Declaration of Competing Interest

On behalf of all authors, the corresponding author states that there is no conflict of interest.

Availability of data and materials

All the data supporting the findings is contained within the manuscript.

Supplementary materials

Supplementary material associated with this article can be found, in the online version, at doi:10.1016/j.jinf.2021.08.025.

References

1. Bicanic T., Meintjes G., Rebe K., et al. Immune reconstitution inflammatory syndrome in HIV associated cryptococcal meningitis: a prospective study. *J Acquir Immune Defic Sydnr* 2009;**51**:130–4.
2. Sungkanuparph S., Filler S.G., Chetchotisakd P., et al. Cryptococcal immune reconstitution inflammatory syndrome after antiretroviral therapy in AIDS patients with cryptococcal meningitis: a prospective multicenter study. *Clin Infect Dis* 2009;**49**:931–4.
3. Barber D.L., Andrade B.B., Sereti I., et al. Immune reconstitution inflammatory syndrome: the trouble with immunity when you had none. *Nature Rev Microbiol* 2012;**10**:150–6.
4. Einsiedel L., Gordon D.L., Dyer J.R.. Paradoxical inflammatory reaction during treatment of Cryptococcus neoformans var. gattii meningitis in an HIV-seronegative woman. *Clin Infect Dis* 2004;**39**(8):78–82.
5. Saag M.S., Graybill R.J., Larsen R.A., et al. Practice guidelines for the management of cryptococcal disease. *Clin Infect Dis* 2000;**30**:710–18.
6. Katchanov J., Branding G., Jefferys L., et al. Neuroimaging of HIV-associated cryptococcal meningitis: comparison of magnetic resonance imaging findings in patients with and without immune reconstitution. *Int J STD AIDS* 2016;**27**(2):110–17.
7. Achenbach C.J., Harrington R.D., Dhanireddy S., et al. Paradoxical immune reconstitution inflammatory syndrome in HIV-infected patients treated with combination antiretroviral therapy after AIDS-defining opportunistic infection. *Clin Infect Dis* 2012;**54**:424–33.
8. Shelburne S.A., Darcourt J., White A.C., et al. The role of immune reconstitution inflammatory syndrome in AIDS-related Cryptococcus neoformans disease in the era of highly active antiretroviral therapy. *Clin Infect Dis* 2005;**40**:1049–52.
9. Perfect J.R., Dismukes W.E., Dromer F., et al. Clinical practice guidelines for the management of cryptococcal disease: 2010 update by the Infectious Diseases Society of America. *Clin Infect Dis* 2010;**50**:291–322.
10. Phillips P., Chapman K., Sharp M., et al. Dexamethasone in Cryptococcus gattii central nervous system infection. *Clin Infect Dis* 2009;**49**(4):591–5.

Yu Yang*
Min Li
Lijuan Yang
Qing Tian

Bing Qin

Department of Neurology, The Third Affiliated Hospital of Sun Yat-Sen University, 600# Tianhe Road, Guangzhou, Guangdong Province 510630, China
*Corresponding author.
E-mail addresses:* yyu@mail.sysu.edu.cn (Y. Yang), plum-min@163.com (M. Li), iamylj@aliyun.com (L. Yang), tianqingsums@163.com (Q. Tian), qinbingsx@aliyun.com (B. Qin)

Genesis, evolution and host species distribution of influenza A (H10N3) virus in China

Dear Editor,

A recent article by Wang in the *Journal of Infection*[1] confirmed the first case of human infection with H10N3 avian influenza virus (AIV) in Zhenjiang, Jiangsu Province, China, in April 2021. Transmission of H10 subtype AIVs from birds to humans is uncommon but has occurred in history. The first reported human infections with an H10 subtype influenza virus occurred in Egypt in 2004.[2] In subsequent surveillance, cross-species transmission of subtype H10 influenza virus has been detected occasionally. The most important of these events were three patients infected with the H10N8 subtype influenza virus and two died in China in 2013.[3] Wang also analyzed the whole genome of the first human-origin H10N3 isolate, indicating that this virus is an avian-origin reassortant strain with the hemagglutinin (HA) and neuraminidase (NA) genes from H10N3 viruses and six internal genes from H9N2 viruses.[1] WHO considered this human case was a sporadic transmission of H10 from avian hosts to humans. However, up to now, there were no same genotype avian-origin H10N3 viruses having been reported.

During our surveillance for AIVs in China, ten H10N3 viruses (Table 1) were isolated from chicken tracheal and cloacal swab samples in live bird markets (LBMs) between December 2019 and May 2021. We sequenced all eight genes of these ten viruses to trace the origin and clarify the genetic properties. The result showed that these avian-origin isolates have a high homology with human-origin strain A/Jiangsu/428/2021. Phylogenetic analysis from sequences available in Global Initiative on Sharing all Influenza Data (GISAID, https://platform.gisaid.org) showed that

H10Nx-HA genes were divided into North America and Eurasian lineages (Figure 1), similar to other HA subtypes of AIVs. In addition, it appears that viruses from the Eurasian lineage are more divergent and have formed several sub-lineages. This ten avian-origin viruses and one human-origin virus belonged to the Eurasian lineage and formed an independent sub-lineage, Group 5 (Figure 1), showing a large evolutionary distance from other H10 strains. In addition, human H10N8 isolated from Jiangxi province in 2013 and 2014 belonged to Group 2 sub-lineage (Figure 1). HyN3 NA genes were divided into three sub-lineages, North America, Eurasian, and Mixed (North America and Eurasian). As shown in Supplementary Figure 1, these novel reassortant H10N3 strains NA belonged to the Eurasian lineage and also formed an independent sub-lineage like the HA segment. Phylogenetic analysis suggested that HA and NA of these H10N3 viruses might have independently evolved a considerably longer time in poultry.

Homology analysis of these avian-origin H10N3 internal genes showed that the polybasic protein 2 (PB2), polybasic protein 1 (PB1), polybasic protein (PA), nucleocapsid protein (NP), matrix protein (M) and nonstructural protein (NS) genes were all derived from H9N2 AIVs. Interestingly, H9N2 AIVs were dominant in LBMs in China in recent years and donate internal genes for human isolates such as H7N9, H10N8 and H5N6.[3-5] This type of AIV with H9N2 derived internal genes attracts the attention of the general public and health professionals in recent years.

We next analyzed the important molecular markers of these avian-origin and human-origin H10N3 strains. From the Supplementary Table, these strains all had G228S mutation at the receptor binding site of the HA protein, indicating a stronger binding capacity for human-like receptor binding.[6] In addition, all strains harbored PB2-A588V, PB1-I368V and PA-K356R mutations, which could enhance polymerase activity, viral replication, and virulence of AIV in mammals.[7-9] Quite unexpectedly, although human-origin and 6 (6/10) avian-origin H10N3 strains contained avian marker PB2-627E, four (4/10) avian-origin isolates contained PB2-E627V mutation, which was found previously to function as an intermediate between 627E and 627K on the H7N9 genetic background.[10] These mammalian molecular markers suggest that these H10N3 viruses may have an even higher capacity for mammalian adaption, especially the strains containing PB2-627V.

Different host species carried distinct major AIV subtypes. We downloaded all the H10 strains information from GISAID database and analyzed their host distribution. As shown in Supplementary Figure 2A, H10 subtype AIVs were mainly isolated from waterfowl (87.50%, 1421/1624), other hosts include terrestrial poultry (6.53%, 106/1624), nonhuman mammals (0.43%, 7/1624) and humans (0.43%, 7/1624). The top three NA subtypes in the H10 strains were N7 (49.75%, 808/1624), N3 (10.16%, 165/1624) and N8 (9.11%, 148/1624). While as shown in Supplementary Figure 2B, H10N3 AIVs were also mainly isolated from waterfowl (88.27%, 143/162),

Table 1
The data of the avian-origin H10N3 isolates in this study.

Strains	Host	Collection date	Collection province	Accession numbers[1]
A/chicken/Jiangsu/0104/2019	chicken	2019.12	Jiangsu	EPI1751735 - EPI1751742
A/chicken/Jiangsu/0110/2019	chicken	2019.12	Jiangsu	EPI1751743 - EPI1751750
A/chicken/Guangxi/HD58/2020	chicken	2020.11	Guangxi	EPI1884738 - EPI1884746
A/chicken/Jiangsu/0178/2021	chicken	2021.01	Jiangsu	EPI1884747 - EPI1884754
A/chicken/Zhejiang/ZJ79/2021	chicken	2021.04	Zhejiang	EPI1884755 - EPI1884762
A/chicken/Zhejiang/HY25/2021	chicken	2021.04	Zhejiang	EPI1884763 - EPI1884770
A/chicken/Jiangsu/HY401/2021	chicken	2021.04	Jiangsu	EPI1884771 - EPI1884778
A/chicken/Jiangsu/JS74/2021	chicken	2021.05	Jiangsu	EPI1884779 - EPI1884786
A/chicken/Zhejiang/HY26/2021	chicken	2021.05	Zhejiang	EPI1884787 - EPI1884794
A/chicken/Zhejiang/0132/2021	chicken	2021.05	Zhejiang	EPI1884795 - EPI1884802

[1] Nucleotide sequences of avian-origin H10N3 isolates were available from Global Initiative on Sharing all Influenza Data (GISAID, https://platform.gisaid.org).
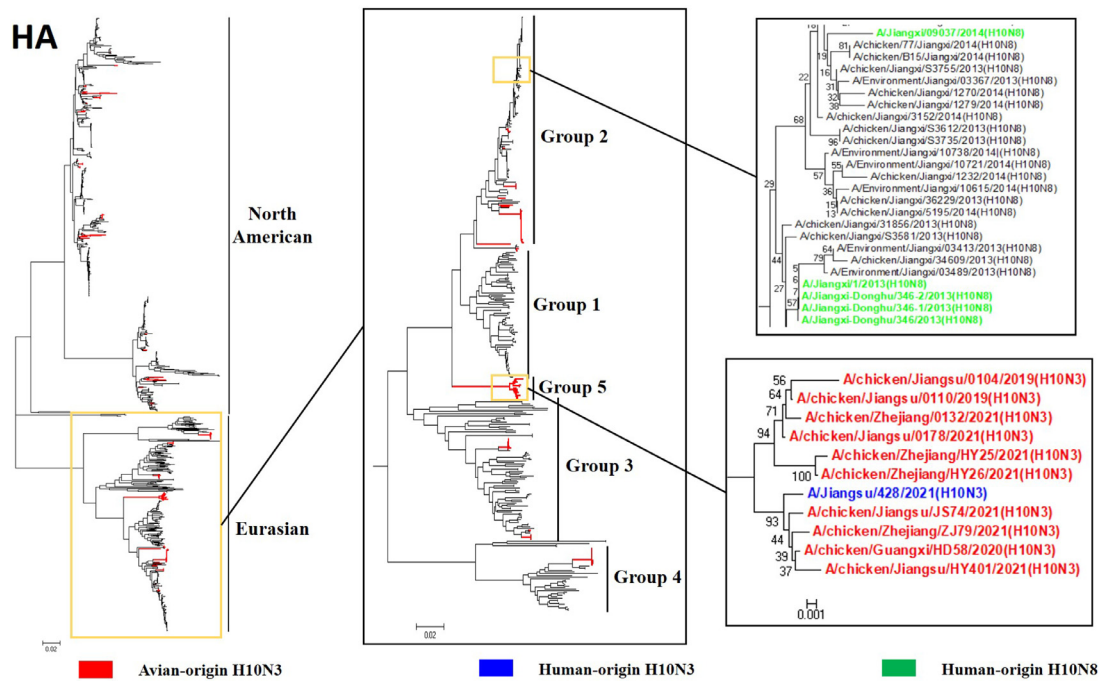
Fig. 1. Phylogenetic trees of H10Nx-HA of AIVs isolated from poultry and download from GISAID database. The ten avian-origin H10N3 isolates were highlighted with red; human-origin H10N3 virus was highlighted with blue; human-origin H10N8 viruses were highlighted with green. The neighbor-joining tree was generated by using MEGA 7 software. The tree was constructed by using the neighbor-joining method with the maximum composite likelihood model in MEGA version 7.0 (http://www.megasoftware.net) with 1,000 bootstrap replicates.

other hosts including chicken (6.17%, 10/162) and humans (0.62%, 1/162). Interestingly, these H10N3 viruses from chicken were all isolated by our laboratory after December 2019 and analyzed in this study. The above data showed that the host of this novel reassortant H10N3 transformed from waterfowl to terrestrial poultry.

In conclusion, these avian-origin H10N3 isolates are highly homologous with human-origin H10N3 strain, and some of them were isolated in Jiangsu Province before human infection, indicating that human infection case was transmitted from poultry to human. These H10N3 isolates internal genes were all derived from H9N2 should arouse our focus, because this type reassortants such as H7N9, H5N6 and H10N8 have caused human infection and death in recent years. Low pathogenic AIVs usually do not cause explicit symptoms in poultry, it might have existed for a long time until we discovered it, which proved by our phylogenetic analysis. In addition, these avian-origin H10N3 isolates with several mammalian molecular markers show an even higher capacity for mammalian adaption. Our findings indicate the importance of continuous surveillance for the emergence and evolution of novel influenza viruses in poultry and the potential threat to public health.

Financial support

Declaration of Competing Interest

No potential conflict of interest was reported by the authors.

Supplementary materials

Supplementary material associated with this article can be found, in the online version, at doi:10.1016/j.jinf.2021.08.021.

References

1. Wang Y, Niu S, Zhang B, Yang C, Zhou Z.. The whole genome analysis for the first human infection with H10N3 influenza virus in China. *J Infect* 2021.
2. Organization PAH.. *Avian influenza virus A (H10N7) circulating among humans in Egypt*. Washington,DC: Pan American Health Organization; 2004.
3. Chen H, Yuan H, Gao R, Zhang J, Wang D, Xiong Y, et al. Clinical and epidemiological characteristics of a fatal case of avian influenza A H10N8 virus infection: a descriptive study. *Lancet* 2014;**383**(9918):714–21.
4. Chen Y, Liang W, Yang S, Wu N, Gao H, Sheng J, et al. Human infections with the emerging avian influenza A H7N9 virus from wet market poultry: clinical analysis and characterisation of viral genome. *Lancet* 2013;**381**(9881):1916–25.
5. Shen YY, Ke CW, Li Q, Yuan RY, Xiang D, Jia WX, et al. Novel reassortant avian influenza A(H5N6) viruses in humans, Guangdong, China, 2015. *Emerg Infect Dis* 2016;**22**(8):1507–9.
6. Zhang Y, Zhao C, Hou Y, Chen Y, Meng F, Zhuang Y, et al. Pandemic threat posed by H3N2 avian influenza virus. *Sci China Life Sci* 2021.
7. Fan S, Hatta M, Kim JH, Halfmann P, Imai M, Macken CA, et al. Novel residues in avian influenza virus PB2 protein affect virulence in mammalian hosts. *Nat Commun* 2014;**5**:5021.
8. Herfst S, Schrauwen EJ, Linster M, Chutinimitkul S, de Wit E, Munster VJ, et al. Airborne transmission of influenza A/H5N1 virus between ferrets. *Science* 2012;**336**(6088):1534–41.
9. Xu W, Sun Z, Liu Q, Xu J, Jiang S, Lu L.. PA-356R is a unique signature of the avian influenza A (H7N9) viruses with bird-to-human transmissibility: potential implication for animal surveillances. *J Infect* 2013;**67**(5):490–494.

10. Luk GS, Leung CY, Sia SF, Choy KT, Zhou J, Ho CC, et al. Transmission of H7N9 influenza viruses with a polymorphism at PB2 residue 627 in chickens and ferrets. *J Virol* 2015;**89**(19):9939–51.

Ruyi Gao
Animal Infectious Disease Laboratory, College of Veterinary Medicine, Yangzhou University, Yangzhou, China
Jiangsu Co-innovation Center for Prevention and Control of Important Animal Infectious Diseases and Zoonosis, Yangzhou University, Yangzhou, Jiangsu, China
Jiangsu Key Laboratory of Zoonosis, Yangzhou, Jiangsu, China

Huafen Zheng
Animal Infectious Disease Laboratory, College of Veterinary Medicine, Yangzhou University, Yangzhou, China

Kaituo Liu
Animal Infectious Disease Laboratory, College of Veterinary Medicine, Yangzhou University, Yangzhou, China
Joint International Research Laboratory of Agriculture and Agri-Product Safety, The Ministry of Education of China, Yangzhou University, Yangzhou, China
Jiangsu Co-innovation Center for Prevention and Control of Important Animal Infectious Diseases and Zoonosis, Yangzhou University, Yangzhou, Jiangsu, China
Jiangsu Key Laboratory of Zoonosis, Yangzhou, Jiangsu, China

Zhuxing Ji, Miao Cai
Animal Infectious Disease Laboratory, College of Veterinary Medicine, Yangzhou University, Yangzhou, China

Min Gu, Jiao Hu, Xiaowen Liu, Shunlin Hu
Animal Infectious Disease Laboratory, College of Veterinary Medicine, Yangzhou University, Yangzhou, China
Jiangsu Co-innovation Center for Prevention and Control of Important Animal Infectious Diseases and Zoonosis, Yangzhou University, Yangzhou, Jiangsu, China
Jiangsu Key Laboratory of Zoonosis, Yangzhou, Jiangsu, China

Xiaoquan Wang*, Xiufan Liu
Animal Infectious Disease Laboratory, College of Veterinary Medicine, Yangzhou University, Yangzhou, China
Joint International Research Laboratory of Agriculture and Agri-Product Safety, The Ministry of Education of China, Yangzhou University, Yangzhou, China
Jiangsu Co-innovation Center for Prevention and Control of Important Animal Infectious Diseases and Zoonosis, Yangzhou University, Yangzhou, Jiangsu, China
Jiangsu Key Laboratory of Zoonosis, Yangzhou, Jiangsu, China

*Corresponding author.
E-mail addresses:* wxq@yzu.edu.cn (X. Wang), xfliu@yzu.edu.cn (X. Liu)